From Diffusion to Magnetization Transfer: A Progressive Journey Through Tissue Microstructure

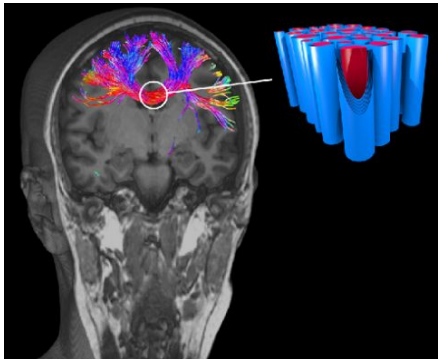

Evgenios Kornaropoulos, PhD

Affiliations:

CRC Human Imaging Group,
University of Liege

CRMBM - CEMEREM,
Aix-Marseille University

Multidimensional diffusion MRI Group,
Lund University

My background


Democritus Univ, Xanthi, Greece

BSc+MSc in Electrical & Computer Engineering


ANT neuro GmbH, Berlin, Germany

Industry experience: EEG acquisition (C++ developer)


Ecole Centrale Paris, Paris, France

PhD on Computer Vision & MRI


University of Cambridge, UK

Research on TBI with 3T DWI


Aix-Marseille Univ, Marseille, France

Microstructural imaging ihMT MRI

TU Delft, The Netherlands

MSc in Biomedical Engineering


Ohio State University, USA

Histopathological Image Analysis


Lund, Sweden

Research on TBI/SLE with UHF-MRI (7T), especially DTI/ DKI



University of Liege, Liege, Belgium

Spinal cord imaging with 3T MRI

…. my scientific parkour

Probing **tissue microstructure** to study neurodegeneration

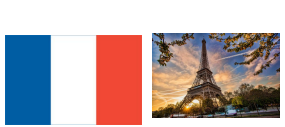

Ecole Centrale Paris, Paris, France

PhD on Computer Vision & MRI

University of Cambridge, UK

Research on TBI with 3T DWI

Aix-Marseille Univ, Marseille, France

Microstructural imaging ihMT MRI

Lund, Sweden

Research on TBI/SLE with UHF-MRI (7T), especially DTI/ DKI

University of Liege, Liege, Belgium

Spinal cord imaging with 3T MRI

Microstructural MRI: seen across scales

Inferring tissue properties at the sub-voxel scale

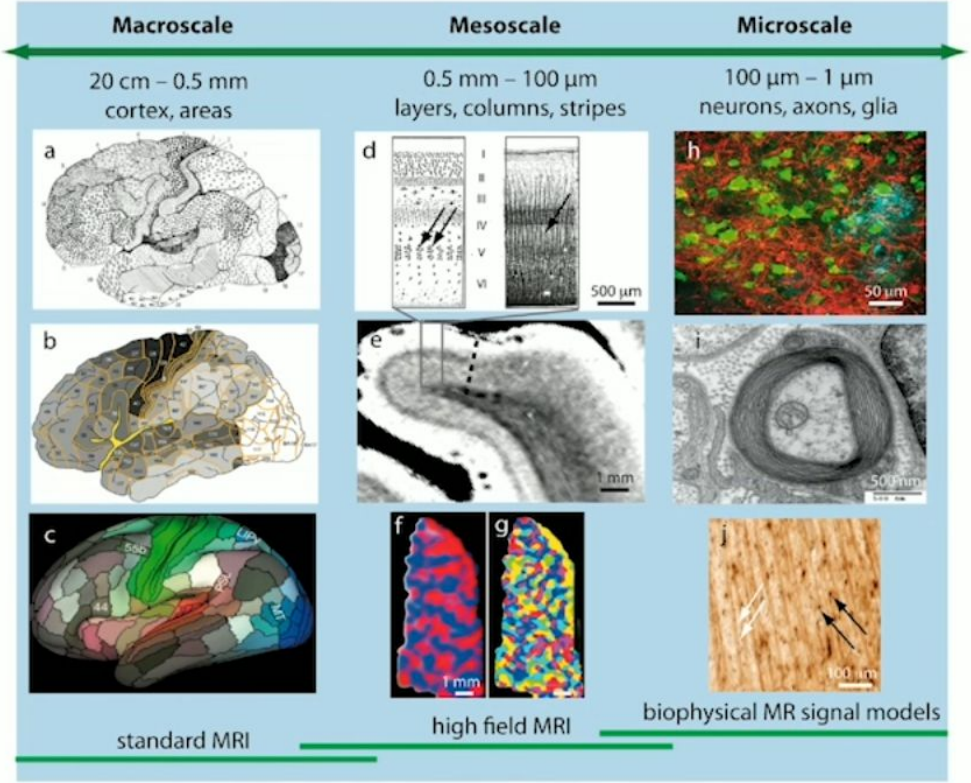

Image modified from Edwards et al., Neuroimage 2018

Microstructural MRI: seen across scales

Inferring tissue properties at the sub-voxel scale

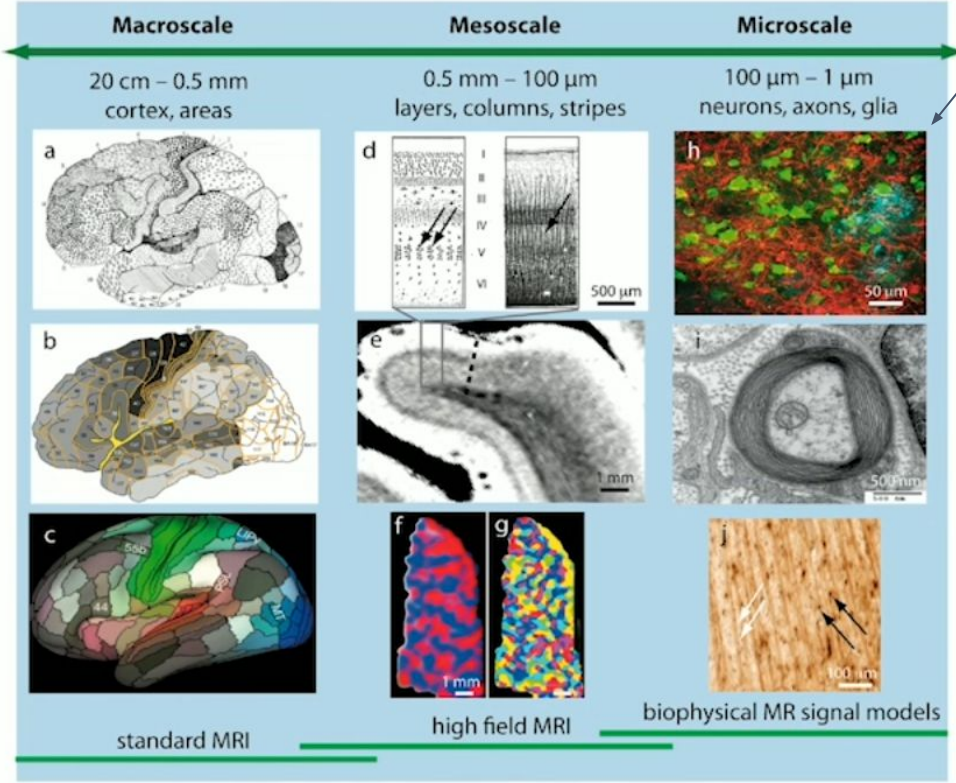

heterogeneous spin systems:

- free water
- macromolecule-bound water
- lipid protons
- protein protons etc

Image modified from Edwards et al., Neuroimage (2018)

Microstructural MRI: seen across scales

Inferring tissue properties at the sub-voxel scale

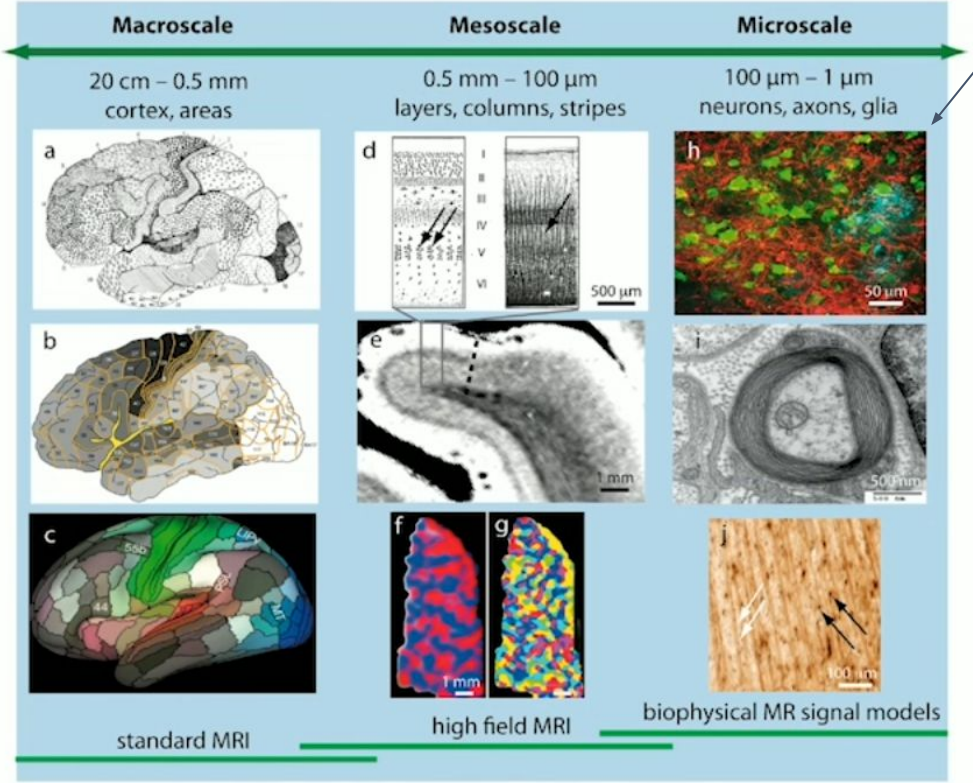

heterogeneous spin systems:

- free water
- macromolecule-bound water
- lipid protons
- protein protons etc

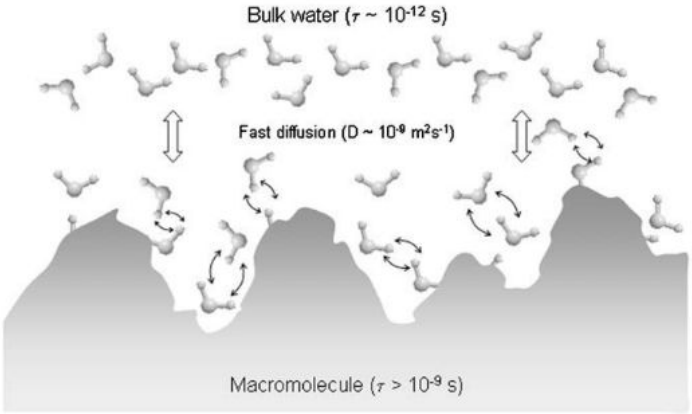

Fig. 1. Schematic representation of a dynamically heterogeneous system.

Image modified from Edwards et al., Neuroimage (2018)

Microstructural MRI: seen across scales

Inferring tissue properties at the sub-voxel scale

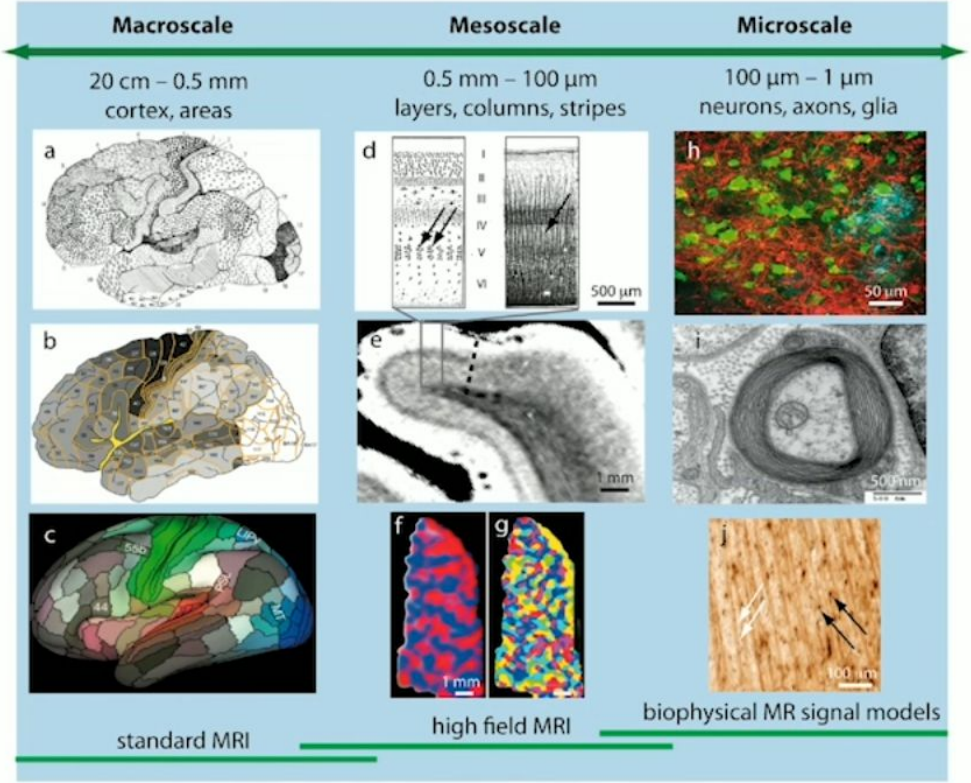

Volume element of the image
On the order of $(0.5 - 1\ mm)^3$

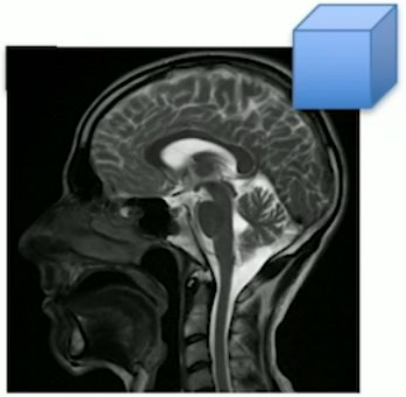

Very active research, many groups
(qMRI, *in vivo* histology, microstructure…)

Goal of microstructural MRI

Goal:
go beyond the voxel level and **<u>infer what's happening at the subvoxel scale.</u>**

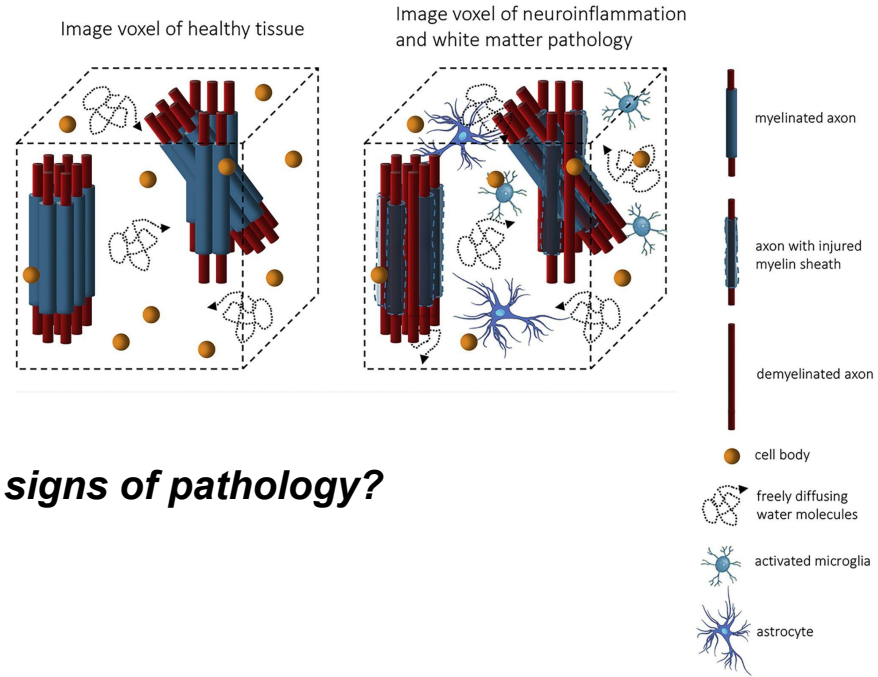

early signs of pathology?

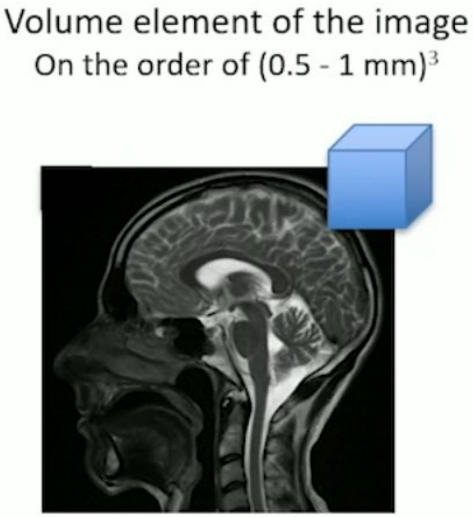

From macro- to micro-

MRI signal mostly detected from **water protons**

Water protons are **local probes** of their microscopic environment (**magnetic sensors**)

Complementary contrast mechanism arises at different scales

Biophysical modeling of the MRI signal consists in **building effective models** for averaged parameters in a bottom-up approach (coarse graining)

Effective MRI model: understand the timescales of fundamental Nuclear Magnetic Resonance properties & the NMR they produce to resonate with the motions occurring in the timescale of interest.

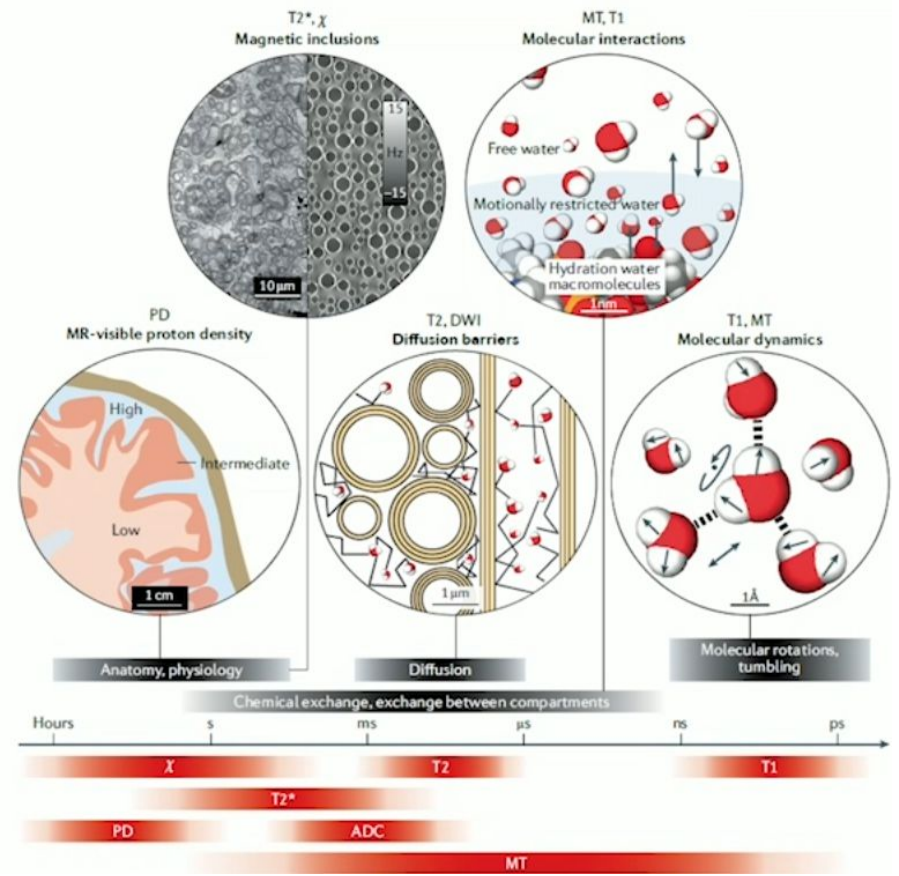

Image modified from Weiskopf et al., Nat Rev Phys (2021)

Molecules within biological tissues

1 mm³

- ➔ **water (around 70%)**
- ➔ cell membranes
- ➔ solute proteins
- ➔ insolute proteins (e.g. myelin)
- ➔ iron
- ➔ metabolites
- ➔ ….

Various compartments

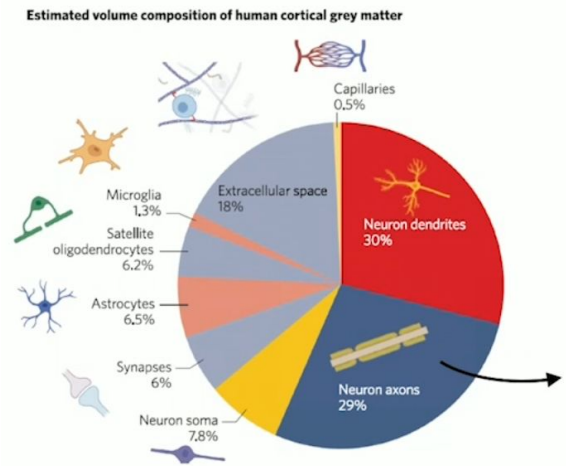

Image modified from Howes et al., Neuropsychopharmacology (2023)

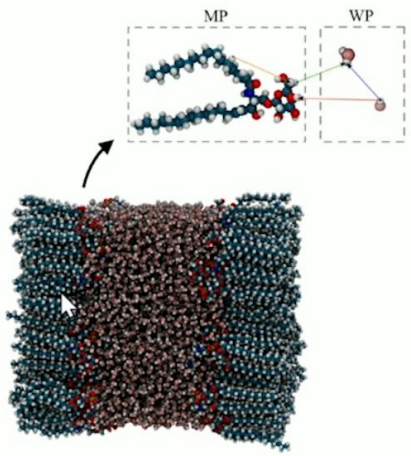

Image modified from Schyboll et al., Sci Report (2019)

Many kinds of protons, molecules and compartments coexists within biological tissues

Molecules within biological tissues

1 mm^3

- ➔ **water (around 70%)**
- ➔ cell membranes
- ➔ solute proteins
- ➔ insolute proteins (e.g. myelin)
- ➔ iron
- ➔ metabolites
- ➔ ….

Various compartments

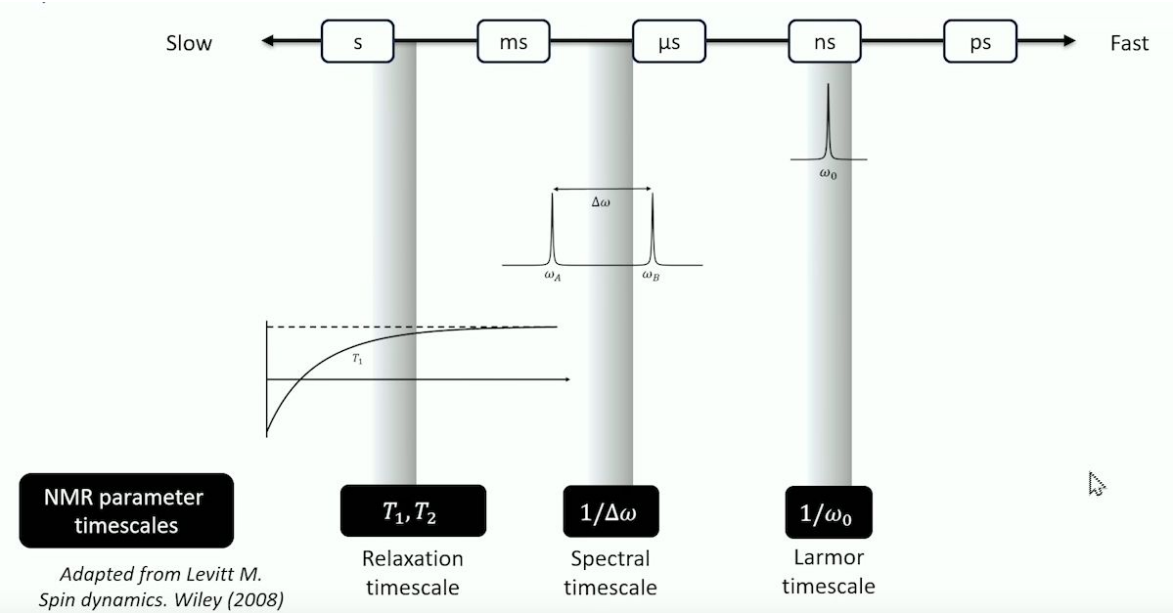

Specific timescales associated with nuclear spin dynamics and magnetic resonance phenomena

Molecules within biological tissues

1 mm³

- ➔ **water (around 70%)**
- ➔ cell membranes
- ➔ solute proteins
- ➔ insolute proteins (e.g. myelin)
- ➔ iron
- ➔ metabolites
- ➔ ….

Various compartments

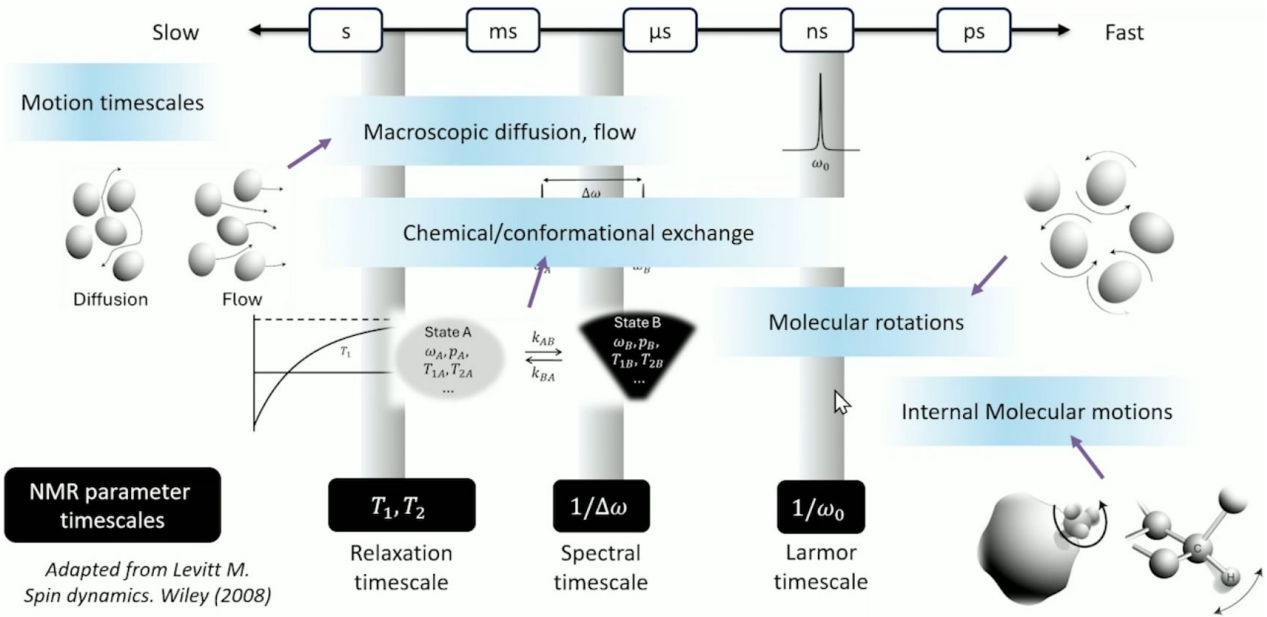

Specific timescales of molecular motion that dominates each environment

Molecules within biological tissues

1 mm³

- ➔ **water (around 70%)**
- ➔ cell membranes
- ➔ solute proteins
- ➔ insolute proteins (e.g. myelin)
- ➔ iron
- ➔ metabolites
- ➔ ….

Various compartments

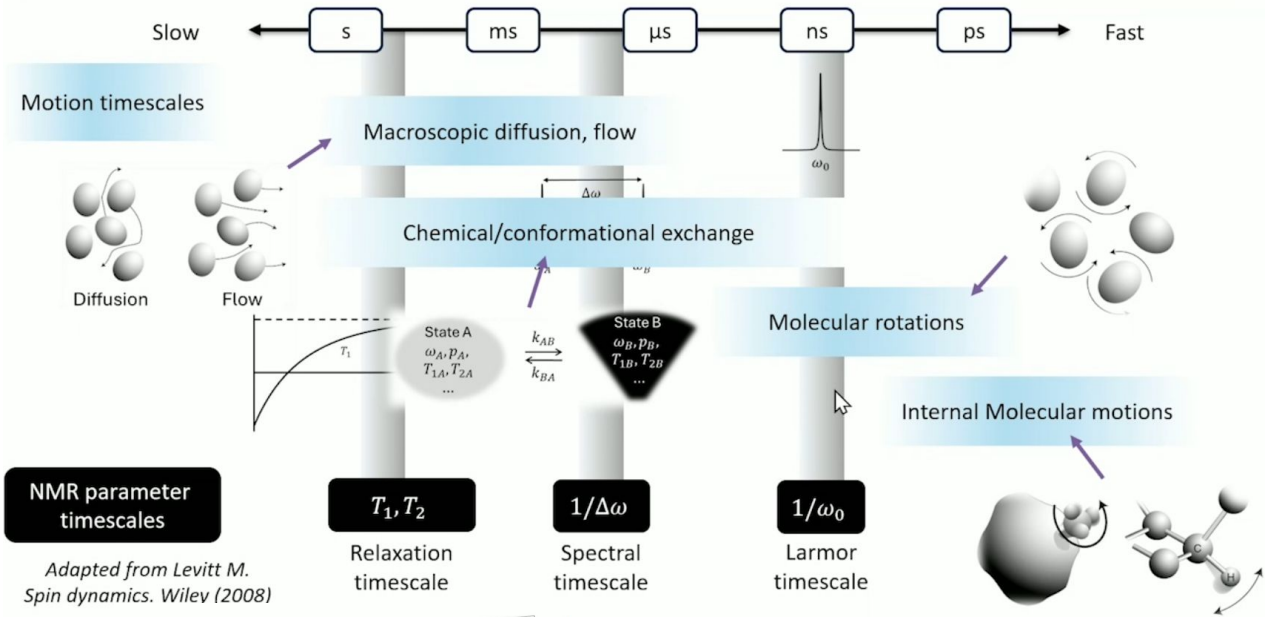

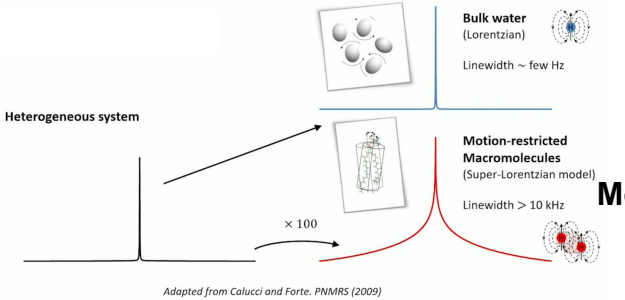

Motionally restricted molecules -> dipole-dipole coupling

Molecules within biological tissues

- ➔ **water (around 70%)**
- ➔ cell membranes -> **DWI**
- ➔ solute proteins -> **CEST**
- ➔ insolute proteins (e.g. myelin) **MT / ihMT**
- ➔ Iron -> **QSM / SWI**
- ➔ Metabolites -> **MRS**
- ➔ ….

Various compartments

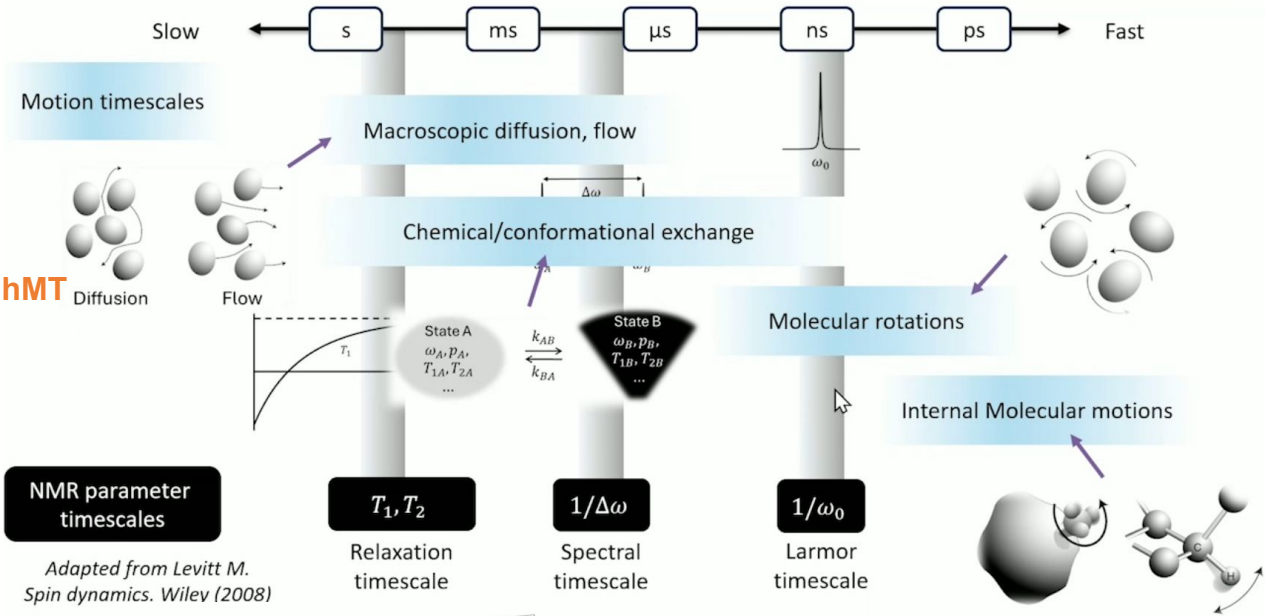

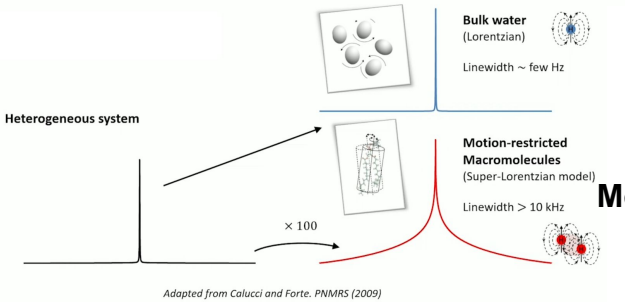

Motionally restricted molecules -> dipole-dipole coupling

Specialized MRI techniques for microstructural imaging

- **DWI,** MT, and **ihMT** are sensitive to **cell membrane properties**
- MT and **ihMT** also probe insoluble proteins (e.g. **myelin**)
- SWI and QSM target iron-bound complexes
- CEST and MRS help us detect low-concentration metabolites

Inhomogeneous Magnetization Transfer

The theory of ihMT:

Nice survey: *Alsop DC, Ercan E, Girard OM, Mackay AL, Michal CA, Varma G, Vinogradov E, Duhamel G. Inhomogeneous magnetization transfer imaging: Concepts and directions for further development. NMR in Biomedicine. 2023 Jun;36(6):e4808.*

ihMT probes:

- dipole-dipole interactions (dipolar order)
- good for imaging myelin

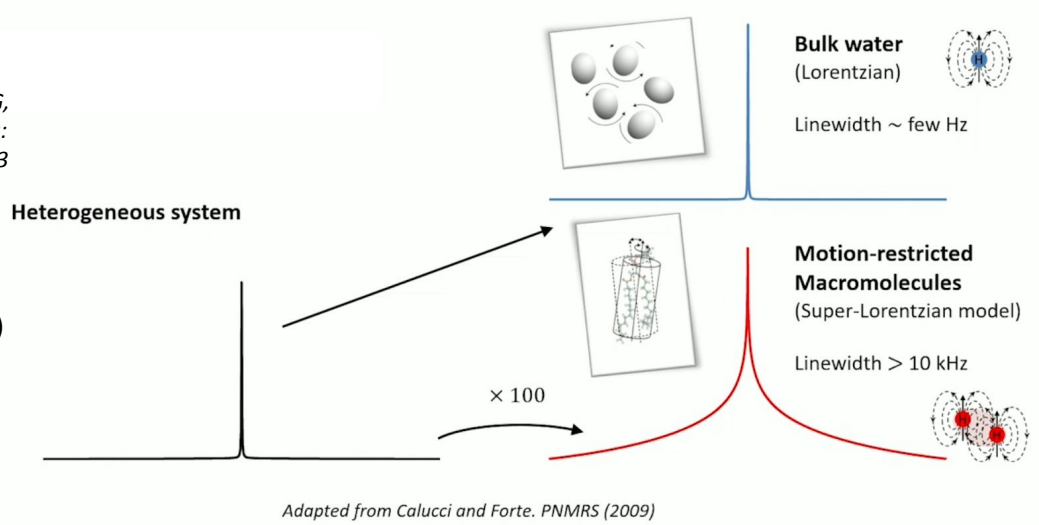

at thermal equilibrium

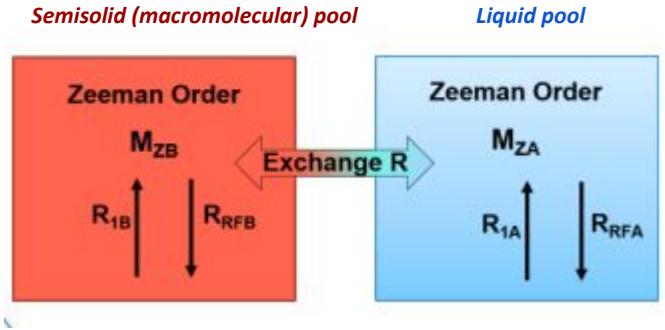

Aix*Marseille université

Inhomogeneous Magnetization Transfer

The theory of ihMT:

Nice survey: *Alsop DC, Ercan E, Girard OM, Mackay AL, Michal CA, Varma G, Vinogradov E, Duhamel G. Inhomogeneous magnetization transfer imaging: Concepts and directions for further development. NMR in Biomedicine. 2023 Jun;36(6):e4808.*

ihMT probes:

- ➢ dipole-dipole interactions (dipolar order)
- ➢ good for imaging myelin

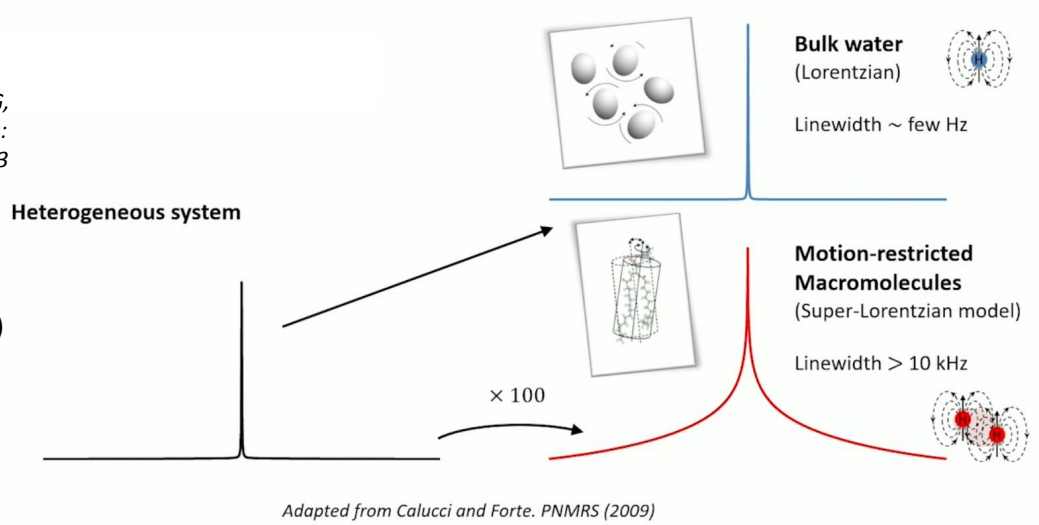

off-resonance RF excitation

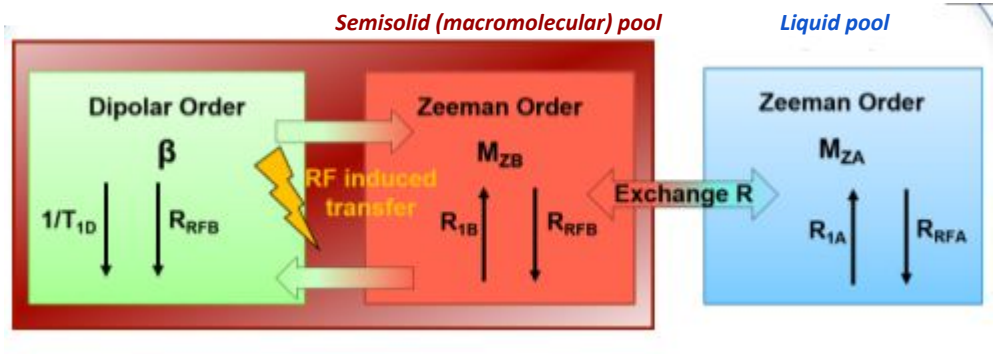

Aix*Marseille université

Inhomogeneous Magnetization Transfer

The theory of ihMT:

Nice survey: *Alsop DC, Ercan E, Girard OM, Mackay AL, Michal CA, Varma G, Vinogradov E, Duhamel G. Inhomogeneous magnetization transfer imaging: Concepts and directions for further development. NMR in Biomedicine. 2023 Jun;36(6):e4808.*

ihMT model

Varma, G., Girard, O.M., Prevost, V.H., Grant, A.K., Duhamel, G. and Alsop, D.C., 2015. Interpretation of magnetization transfer from inhomogeneously broadened lines (ihMT) in tissues as a dipolar order effect within motion restricted molecules. Journal of magnetic resonance, 260, pp.67-76.

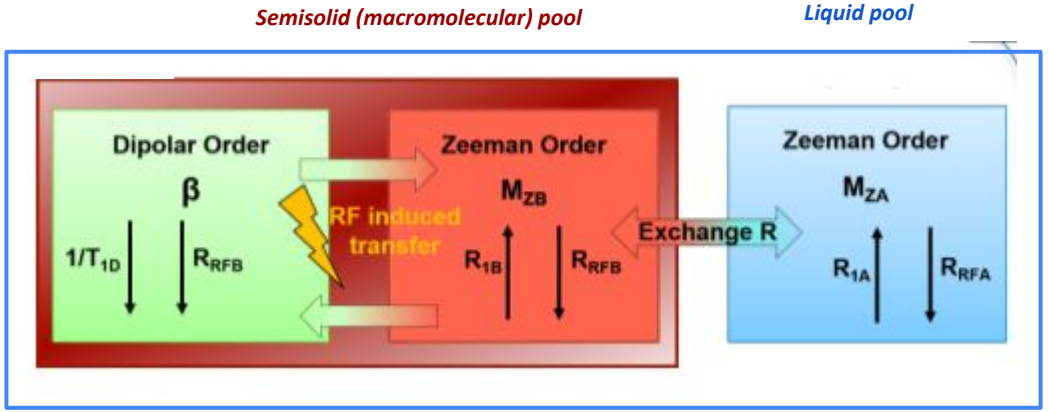

- ***R1f:*** *longitudinal relaxation rate of the free pool*
- ***T2f:*** *transverse relaxation time of the free pool*
- ***T2b:*** *transverse relaxation time of the bound pool*
- ***R:*** *exchange rate*
- ***M0b:*** *equilibrium magnetization of the bound pool*
- ***T1d:*** *longitudinal relaxation time in the presence of dipolar interaction*

Inhomogeneous Magnetization Transfer

The theory of ihMT:

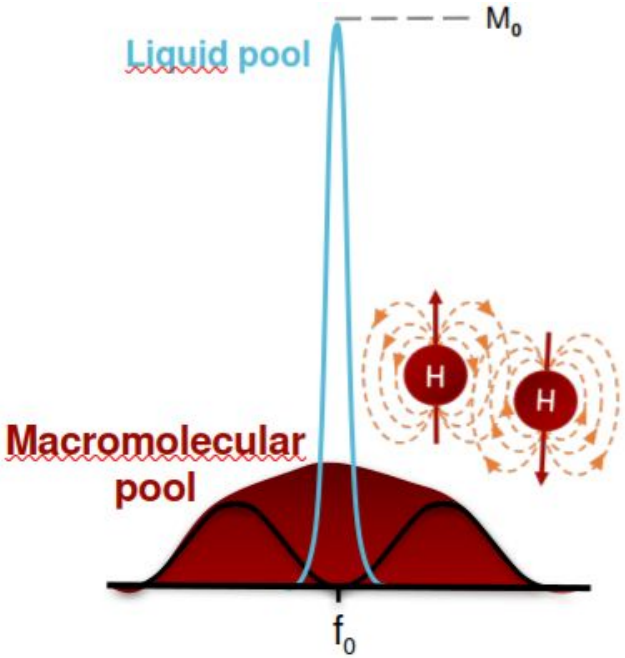

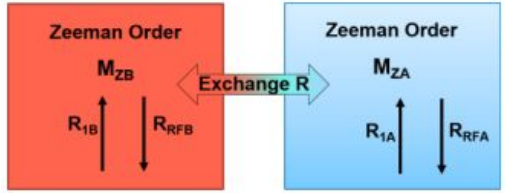

Inhomogeneous Magnetization Transfer

The theory of ihMT:

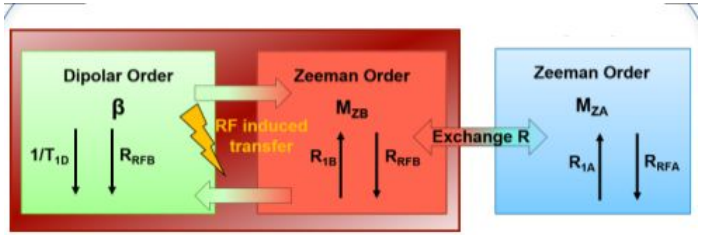

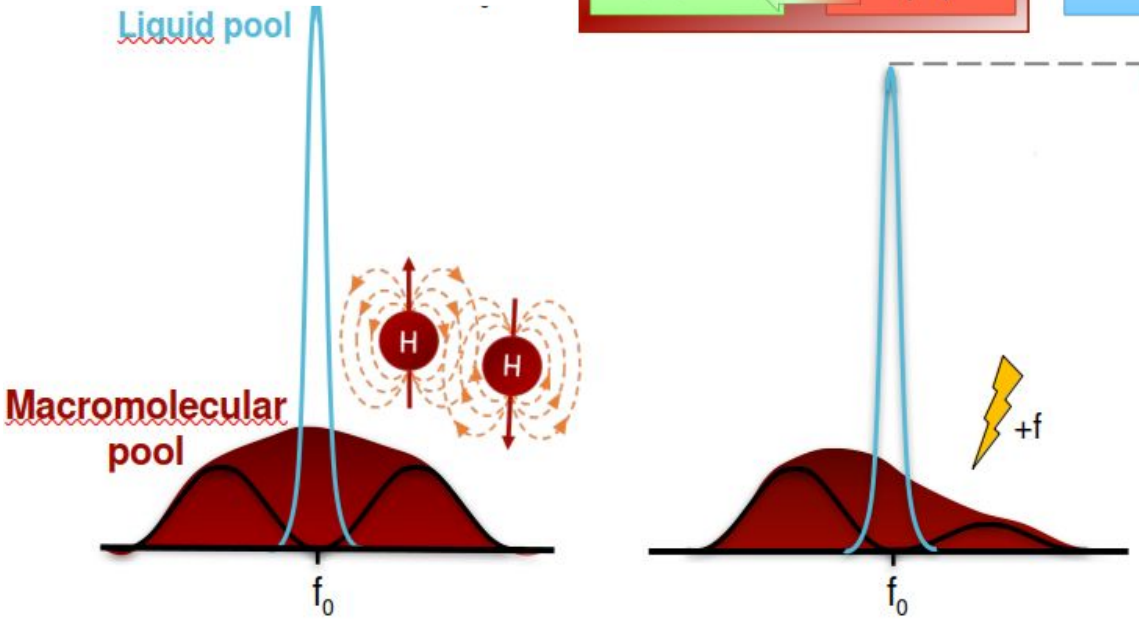

Inhomogeneous Magnetization Transfer

The theory of ihMT:

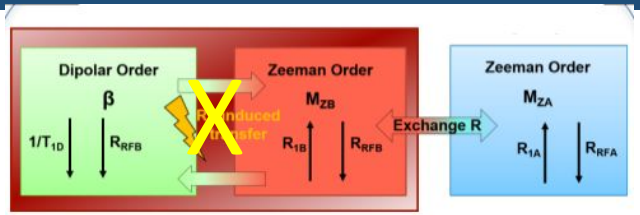

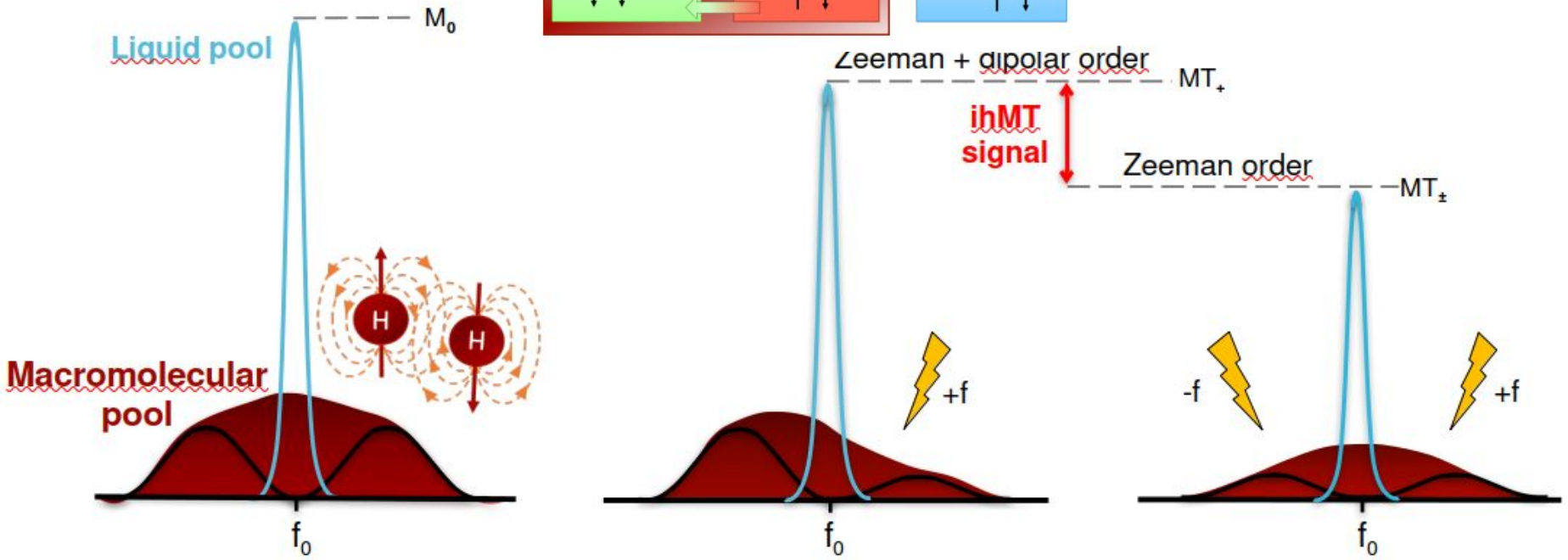

Inhomogeneous Magnetization Transfer

The theory of ihMT:

$$ihMTR = \frac{S_+ + S_- - 2S_\pm}{S_0},$$

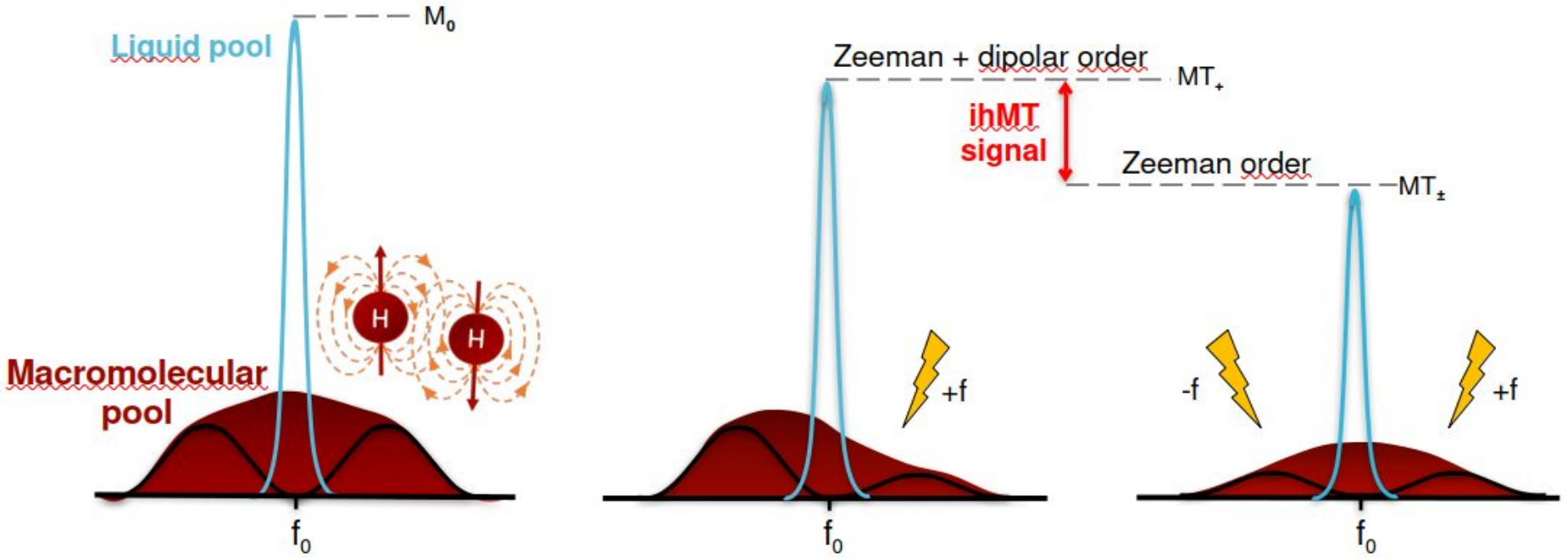

Inhomogeneous Magnetization Transfer for myelin imaging

Our results: **myelin imaging via ihMT**

presented at the
ISMRM 2024 conference
in the process towards publication…

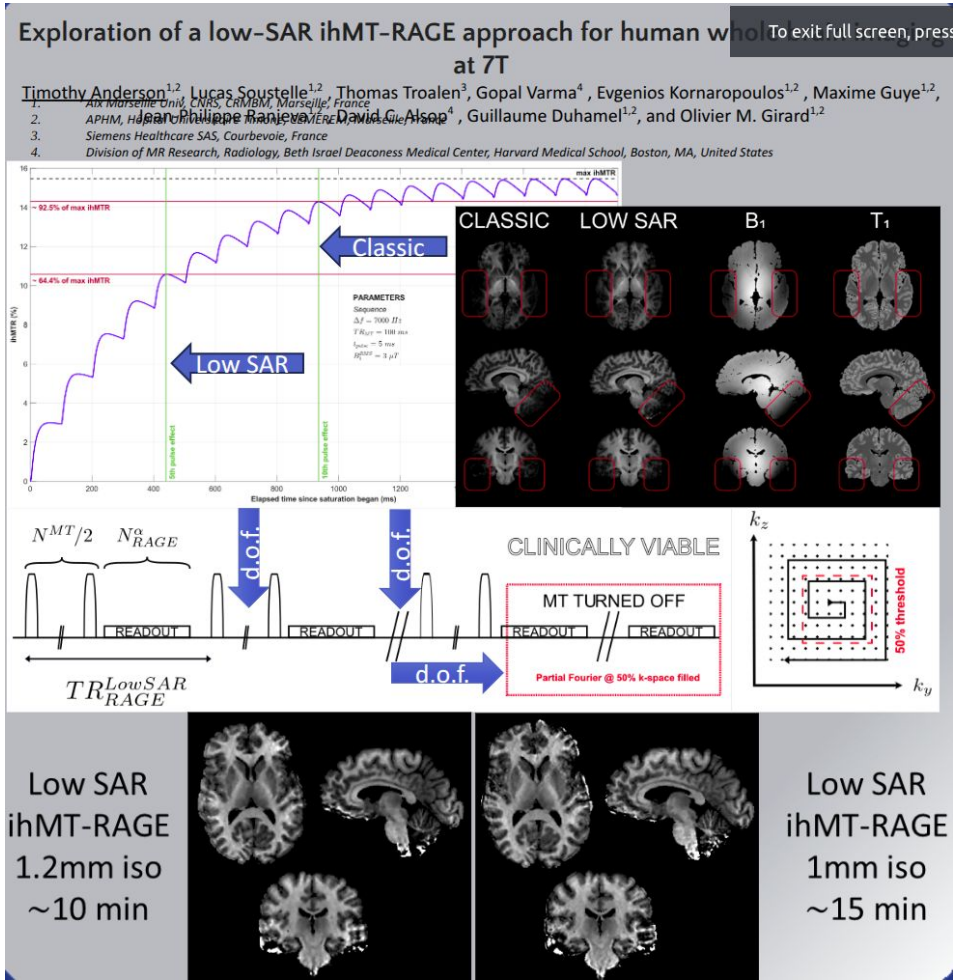

Inhomogeneous Magnetization Transfer for cardiac imaging

The Cardiac Conduction System (CCS) regulates normal heartbeat
of its normal pattern (e.g. ventricular fibrillation) could cause sudden cardiac death

★ **Purkinje Fibers (PF)**
could initiate **ventricular fibrillation**

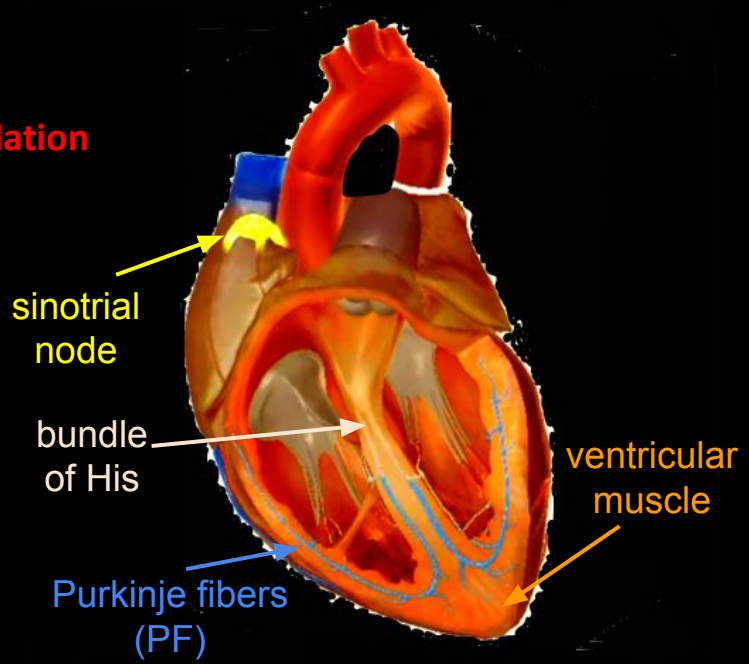

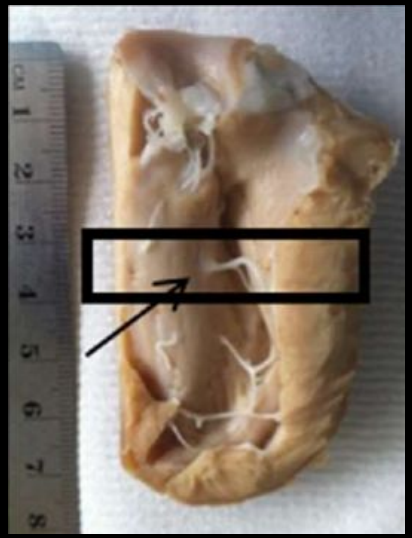

Inhomogeneous Magnetization Transfer for cardiac imaging

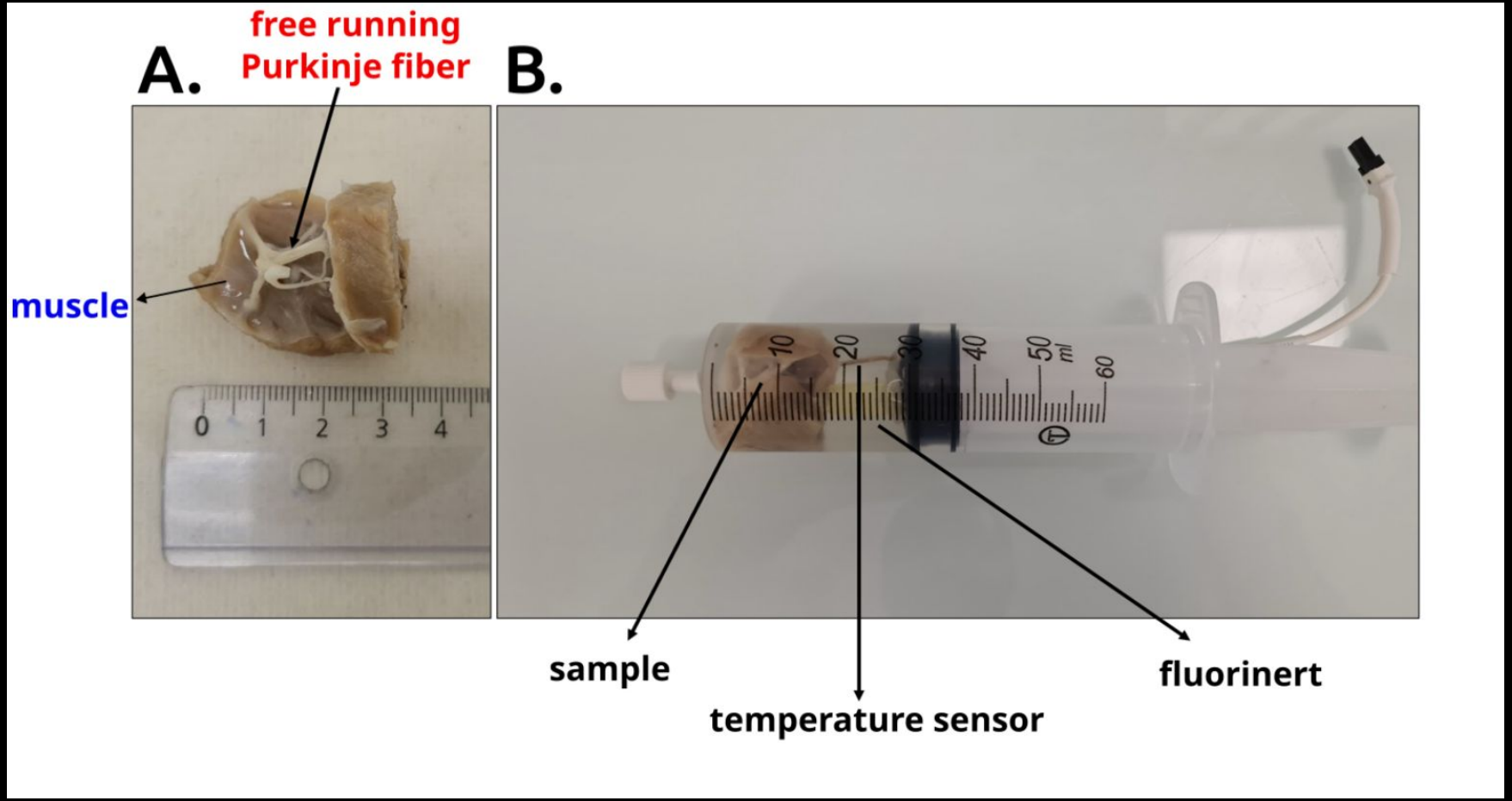

Inhomogeneous Magnetization Transfer for cardiac imaging

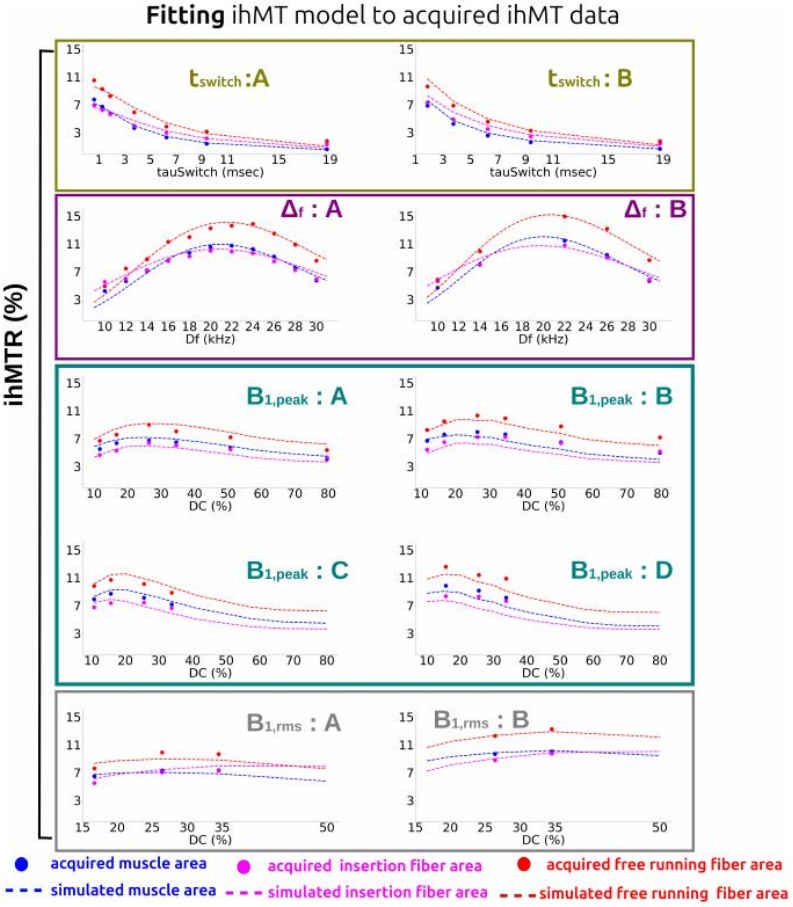

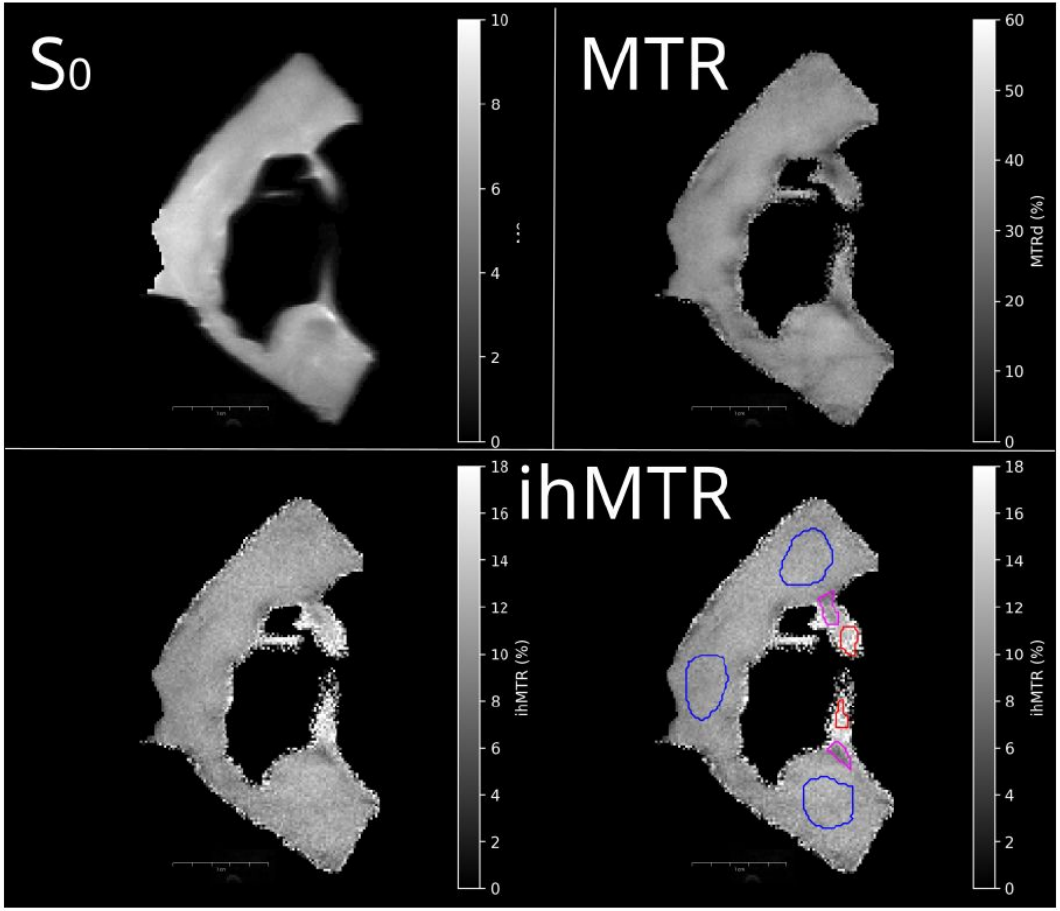

Inhomogeneous Magnetization Transfer for cardiac imaging

The ihMT biophysical parameters	Predefined range of values	Mean value & Std ($muscle$, $fiber_{insertion}$, $fiber_{free}$)
M_0^A	-	1.00, 1.00, 1.00
$R_1^A(s^{-1})$	[0.001, 5]	**3.34 ± 1.65**, **4.36 ± 0.03**, **3.73 ± 0.12**
$T_2^A(ms)$	[1, 5000]	**1.09 ± 0.36**, **2.34 ± 0.33**, **1.52 ± 0.14**
R	[0.01, 100]	**40.04 ± 10.96** , **21.62 ± 0.16**, **30.33 ± 1.46**
M_0^B	[0.1, 50]	**5.73 ± 2.91**, **3.99 ± 0.28**, **6.14 ± 0.53**
$R_1^B(s^{-1})$	-	0.99, 0.99, 0.99
$T_2^B(\mu s)$	[3, 20]	**7.20 ± 0.13**, **7.42 ± 0.17**, **7.62 ± 0.13**
$T_{1D}(ms)$	[0.001, 50]	**2.03 ± 0.20**, **4.51 ± 0.65**, **3.28 ± 0.35**

Inhomogeneous Magnetization Transfer for cardiac imaging

Conclusions on that study:

- via fitting acquired data -> **a cardiac ihMT model**
- higher T1D values in PF compared to muscle
- lower exchange rate in PF compared to muscle
- **better contrast in ihMT compared to T2w or MT**

presented at the
ISMRM 2024 conference
in the process towards publication…

ORIGINAL ARTICLE
Journal Section

Inhomogeneous Magnetization transfer (ihMT) as an alternative source of MRI contrast for the cardiac conduction system: ex-vivo assessment of the ihMT biophysical model in differentiating cardiac muscle from Purkinje fibers

Evgenios N. Kornaropoulos, PhD[1*†] | Arash Forodighasemabadi, PhD[2†] | Lucas Soustelle, PhD[1] | Timothy Andersson[1] | Bruno Quesson, PhD[2,3] | Gopal Varma, PhD[4] | David Alsop, PhD[4] | Olivier Girard, PhD[1‡] | Julie Magat, PhD[2,3‡] | Guillaume Duhamel, PhD[1‡]

[1]Aix-Marseille Univ, CNRS, CRMBM, Marseille, France
[2]IHU LIRYC, Univ of Bordeaux, Pessac, France
[3]CRMSB, UMR 5536 CNRS/Université de Bordeaux, Bordeaux, France
[4]Department of Radiology, Beth Israel Deaconess Medical Center and Harvard Medical School, Boston, Massachusetts, USA

Correspondence
Evgenios N. Kornaropoulos PhD, Center for Magnetic Resonance in Biology and Medicine, Aix-Marseille University, Marseille, France
Email: ekornaropoulos@uliege.be

Abstract

Imaging of the cardiac conduction system for the prevention and treatment of lethal arrhythmias is of high importance. Nonetheless, such an endeavour remains challenging, since conventional structural MRI (i.e. T1w, T2w and proton density) has not managed to provide good contrast between the cardiac muscles and one of the main components of the cardiac conduction system: the Purkinje network of fibers within the myocardium, that regulate ventricular electrical impulse formation and conduction. Instead, inhomogeneous Magnetization Transfer (ihMT) shows great

liryc
L'institut des maladies du rythme cardiaque

Aix*Marseille université
Socialement engagée

HARVARD MEDICAL SCHOOL

Diffusion Tensor and Diffusion Kurtosis Imaging

Main lines of research in DWI:

Diffusion encoding strategy

- FEXI (isolate exchange)
- Free-waveform DWI (flexible sensitivity to microstructure)
- Tensor-values DWI
  - Linear Tensor Encoding (LTE)
  - Spherical Tensor Encoding (STE)
  - Planar Tensor Encoding (PTE)

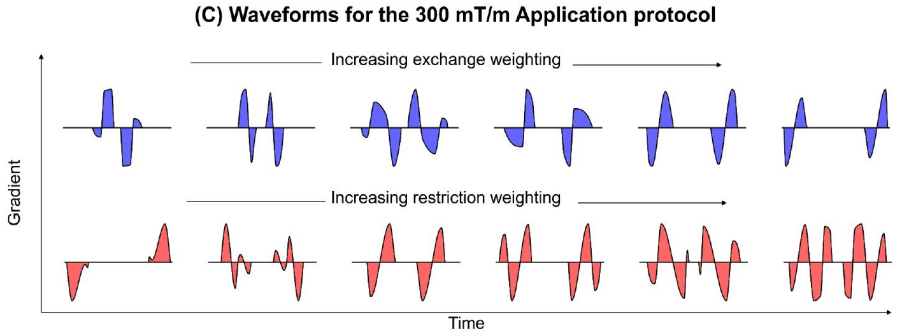

Chakwizira et al., Neuroimage (2023)

Biophysical modelling

- DTI
- DKI
- NODDI
- CHARMED
- SANDI
- NEXI
- CEXI

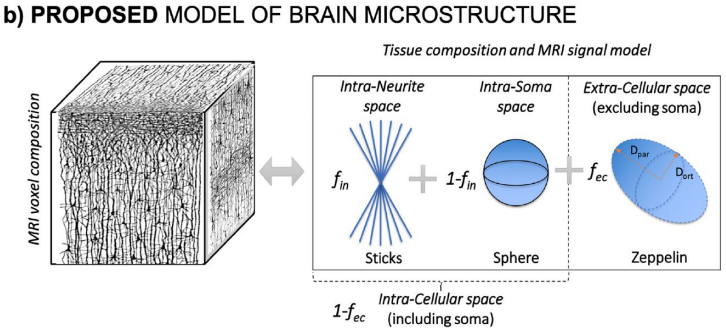

Palombo et al., Neuroimage (2020) - SANDI

Diffusion Tensor and Diffusion Kurtosis Imaging

Main lines of research in DWI:

Diffusion encoding strategy

- FEXI (isolate exchange)
- Free-waveform DWI (flexible sensitivity to microstructure)
- Tensor-values DWI
  - Linear Tensor Encoding (LTE)
  - Spherical Tensor Encoding (STE)
  - Planar Tensor Encoding (PTE)

Biophysical modelling

- DTI
- DKI
- NODDI
- CHARMED
- SANDI
- NEXI
- CEXI

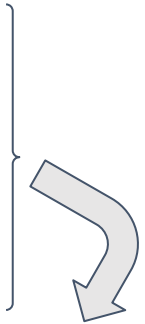

Pulsed Gradient Spin Echo (PGSE)

Diffusion Tensor and Diffusion Kurtosis Imaging

Main lines of research in DWI:

Diffusion encoding strategy

- FEXI (isolate exchange)
- Free-waveform DWI (flexible sensitivity to microstructure)
- Tensor-values DWI
  - Linear Tensor Encoding (LTE)
  - Spherical Tensor Encoding (STE)
  - Planar Tensor Encoding (PTE)

Biophysical modelling

- **DTI**
- **DKI**
- NODDI
- CHARMED
- SANDI
- NEXI
- CEXI

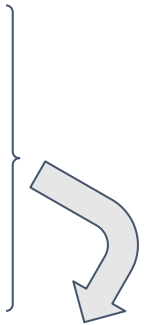

Pulsed Gradient Spin Echo (PGSE)

Diffusion Tensor and Diffusion Kurtosis Imaging

2 different pathologies in neurodegeneration:

Systemic Lupus Erythematosus (SLE)

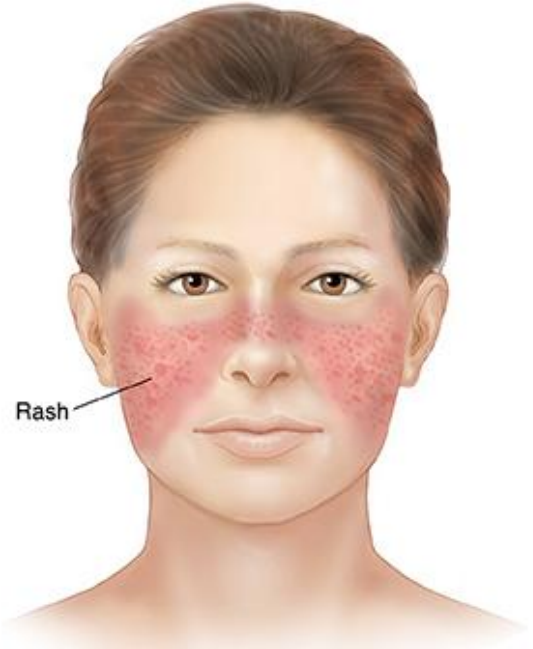

Traumatic Brain Injury (TBI)

Diffusion Tensor and Diffusion Kurtosis Imaging

2 different pathologies in neurodegeneration:

Systemic Lupus Erythematosus (SLE)

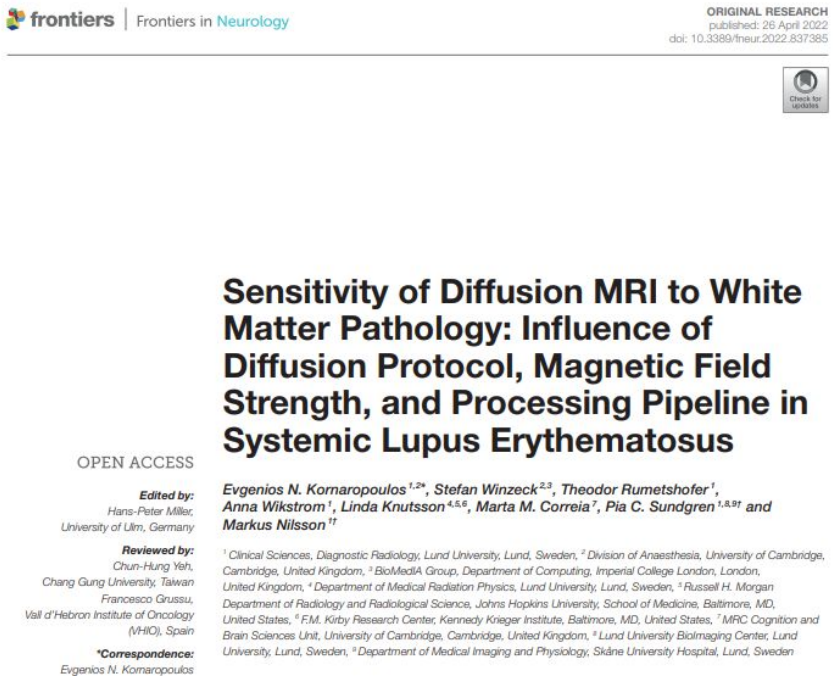

frontiers | Frontiers in Neurology

ORIGINAL RESEARCH
published: 26 April 2022
doi: 10.3389/fneur.2022.837385

Check for updates

Sensitivity of Diffusion MRI to White Matter Pathology: Influence of Diffusion Protocol, Magnetic Field Strength, and Processing Pipeline in Systemic Lupus Erythematosus

OPEN ACCESS

Evgenios N. Kornaropoulos[1,2], Stefan Winzeck[2,3], Theodor Rumetshofer[1], Anna Wikstrom[1], Linda Knutsson[4,5,6], Marta M. Correia[7], Pia C. Sundgren[1,8,9†] and Markus Nilsson[1†]*

[1] Clinical Sciences, Diagnostic Radiology, Lund University, Lund, Sweden, [2] Division of Anaesthesia, University of Cambridge, Cambridge, United Kingdom, [3] BioMedIA Group, Department of Computing, Imperial College London, London, United Kingdom, [4] Department of Medical Radiation Physics, Lund University, Lund, Sweden, [5] Russell H. Morgan Department of Radiology and Radiological Science, Johns Hopkins University, School of Medicine, Baltimore, MD, United States, [6] F.M. Kirby Research Center, Kennedy Krieger Institute, Baltimore, MD, United States, [7] MRC Cognition and Brain Sciences Unit, University of Cambridge, Cambridge, United Kingdom, [8] Lund University BioImaging Center, Lund University, Lund, Sweden, [9] Department of Medical Imaging and Physiology, Skåne University Hospital, Lund, Sweden

Edited by:
Hans-Peter Müller,
University of Ulm, Germany

Reviewed by:
Chun-Hung Yeh,
Chang Gung University, Taiwan
Francesco Grussu,
Vall d'Hebron Institute of Oncology (VHIO), Spain

***Correspondence:**
Evgenios N. Kornaropoulos

Traumatic Brain Injury (TBI)

Journal of Neurotrauma
39:829–840 (June 2022)
Mary Ann Liebert, Inc.
DOI: 10.1089/neu.2021.0447

Journal of Neurotrauma

Open camera or QR reader and scan code to access this article and other resources online.

ORIGINAL ARTICLE — CLINICAL STUDIES

Post-Concussive Vestibular Dysfunction Is Related to Injury to the Inferior Vestibular Nerve

Anna Gard[1,*] Ali Al-Husseini[1] Evgenios N. Kornaropoulos[2] Alessandro De Maio[3] Yelverton Tegner[4] Isabella Björkman-Burtscher[5] Karin Markenroth Bloch[6] Markus Nilsson[2] Måns Magnusson[7] and Niklas Marklund[1]

Journal of Neurotrauma
41:1533–1549 (July 2024)
Mary Ann Liebert, Inc.
DOI: 10.1089/neu.2023.0099

Journal of Neurotrauma

Open camera or QR reader and scan code to access this article and other resources online.

ORIGINAL ARTICLE — IMAGING

Widespread White Matter Abnormalities in Concussed Athletes Detected by 7T Diffusion Magnetic Resonance Imaging

Diffusion Tensor and Diffusion Kurtosis Imaging

SLE study

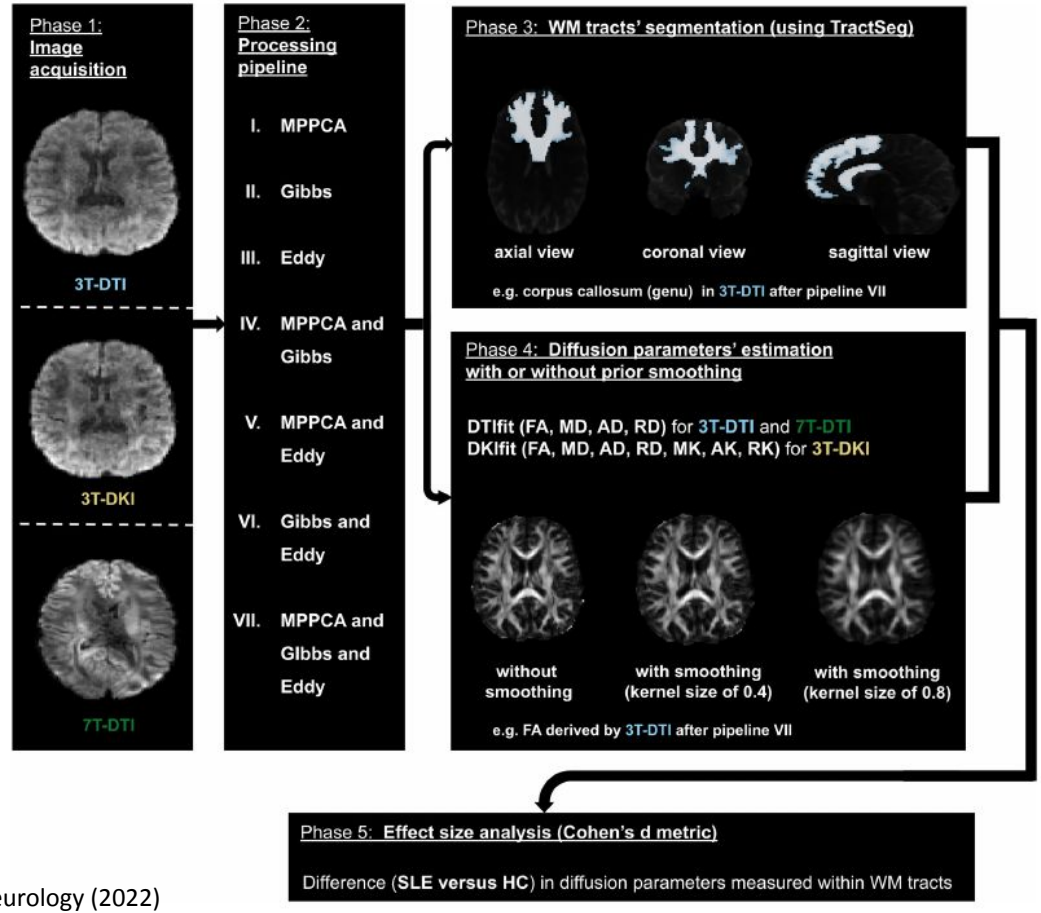

Kornaropoulos et al., frontiers in Neurology (2022)

Diffusion Tensor and Diffusion Kurtosis Imaging

SLE study

TABLE 1 | Demographics and image acquisition parameters.

Image acquisition	#SLE, #HC	Mean age (std) of HC, SLE	Image resolution (isotropic, in mm^3)	*b*-values in s/mm^2 (# of directions)	TR/TE in ms/ms
3T-DTI	63, 20	37 (9) , 36 (9)	2.0	0 (8), 1,000 (64)	7,300/73
3T-DKI	56, 20	37 (9) , 35 (9)	2.3	0 (3), 250 (6), 500 (6), 1,000 (20), 2750 (30)	7,500/103
7T-DTI	54, 21	40 (10) , 40 (9)	2.0	0 (3), 1,000 (30)	8,816/62

Rows show the three protocols: # corresponds to the number of, SLE, patients with systemic lupus erythematosus; HC, human controls; TR, repetition time; TE, echo time. In total 106 subjects participated in this study: 76 patients with SLE and 30 HC. Out of the 106 subjects, 47 were scanned with all three image acquisition protocols (3T-DTI and 3T-DKI and 7T-DTI): 37 patients with SLE and 10 HC.

Kornaropoulos et al., frontiers in Neurology (2022)

Diffusion Tensor and Diffusion Kurtosis Imaging

SLE study

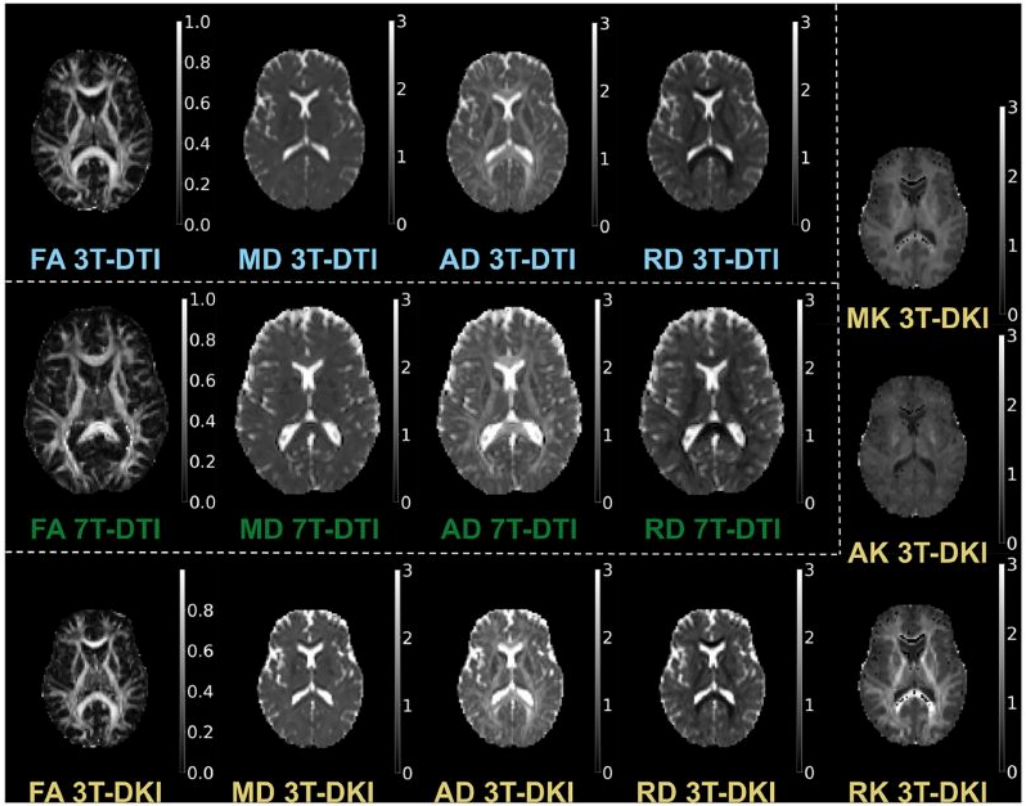

Kornaropoulos et al., frontiers in Neurology (2022)

Diffusion Tensor and Diffusion Kurtosis Imaging

SLE study

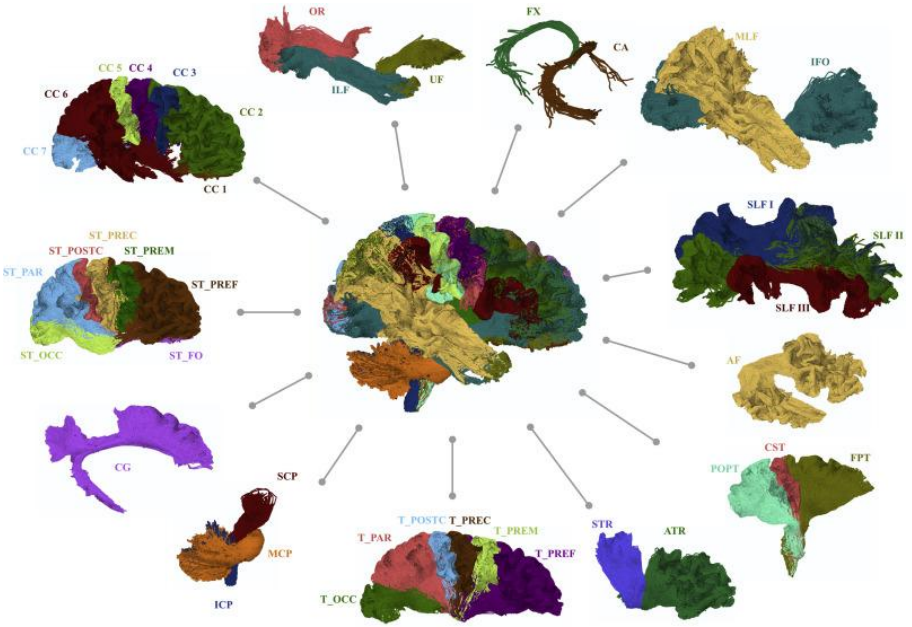

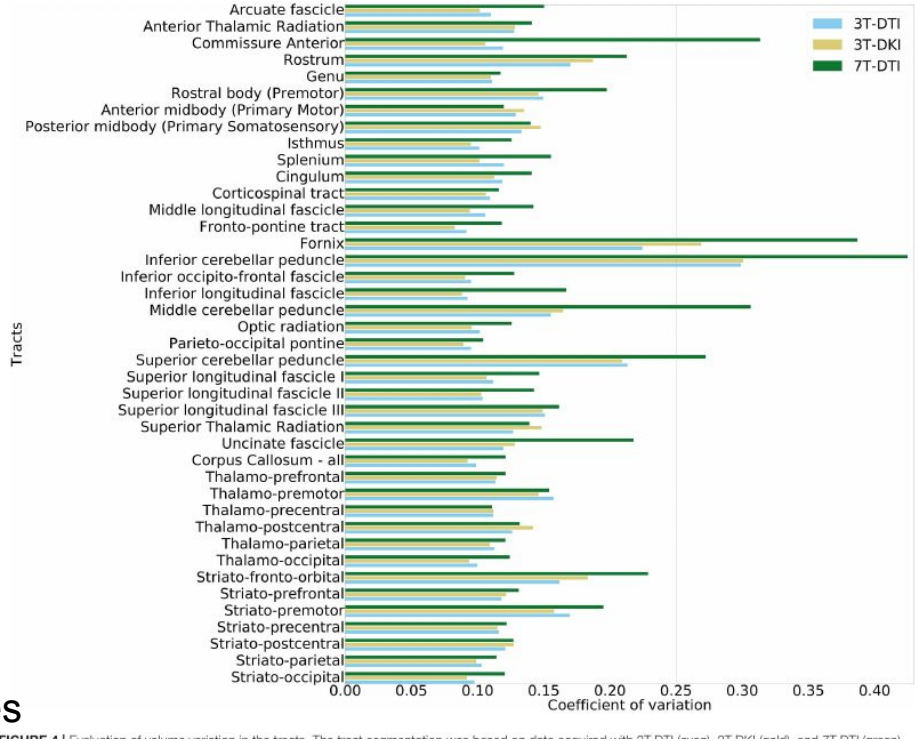

TractSeg (Deep Learning): 72 white matter bundles automatic segmentation

Kornaropoulos et al., frontiers in Neurology (2022)

Diffusion Tensor and Diffusion Kurtosis Imaging

SLE study

Pipelines comparison:

- **minuscule differences** across the data processing pipelines
- correcting for distortions from motion and eddy currents (**Eddy**) was **the most beneficial**

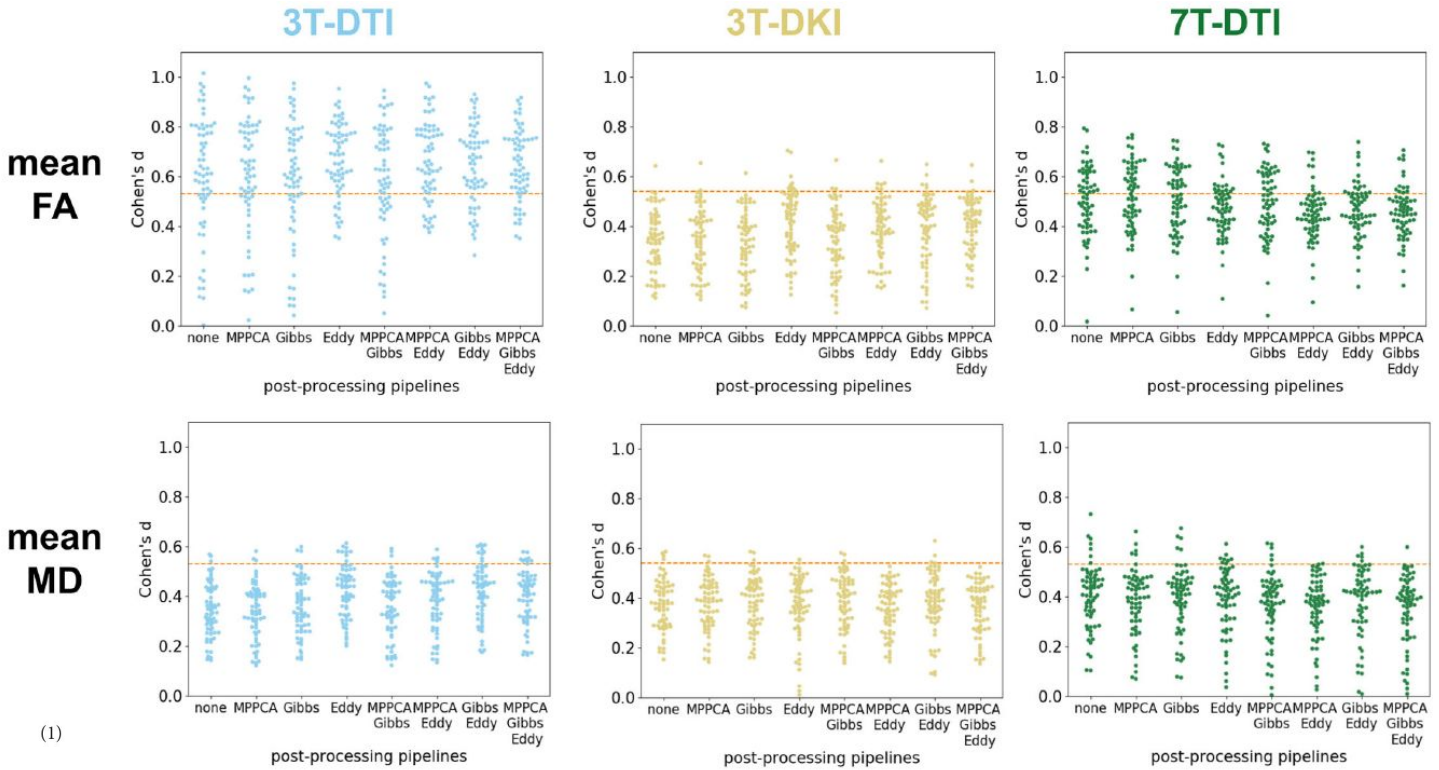

$$d = (u_{HC} - u_{SLE})/s \quad (1)$$

with

$$s = \sqrt{((n_{HC} - 1)s_{HC}^2 + (n_{SLE} - 1)s_{SLE}^2)/(n_{HC} + n_{SLE} - 2)} \quad (2)$$

Kornaropoulos et al., frontiers in Neurology (2022)

Diffusion Tensor and Diffusion Kurtosis Imaging

SLE study

Pipelines comparison:

- minuscule differences across the data processing pipelines
- correcting for distortions from motion and eddy currents (Eddy) was the most beneficial
- **gross smoothing reduced effect sizes** by up to 20% !

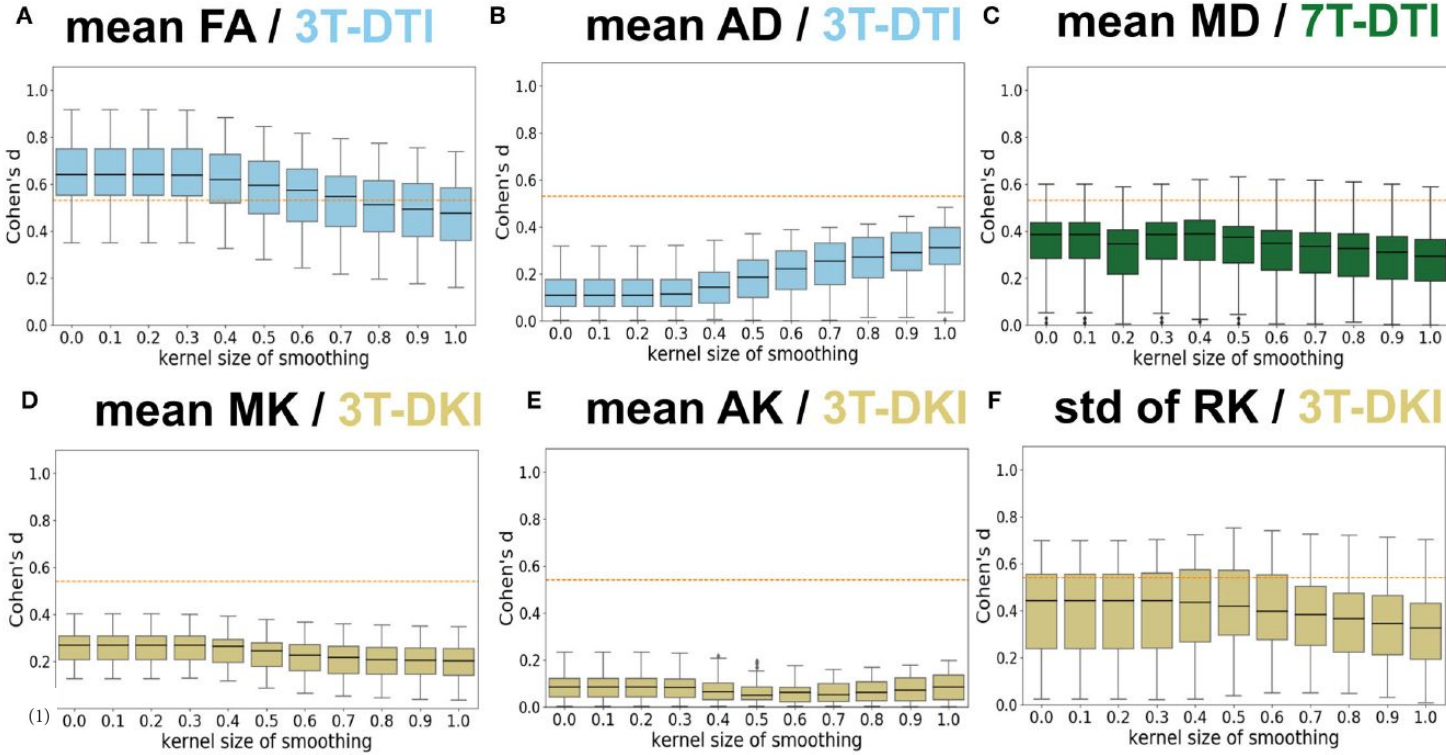

$$d = (u_{HC} - u_{SLE})/s \quad (1)$$

with

$$s = \sqrt{((n_{HC} - 1)s_{HC}^2 + (n_{SLE} - 1)s_{SLE}^2)/(n_{HC} + n_{SLE} - 2)} \quad (2)$$

Kornaropoulos et al., frontiers in Neurology (2022)

Diffusion Tensor and Diffusion Kurtosis Imaging

SLE study

Diffusion protocols & magnetic field strength comparison:

- the **diffusion protocol** had the strongest influence on effect sizes among the ones examined
- **DKI is less sensitive than DTI** to WM pathology in SLE

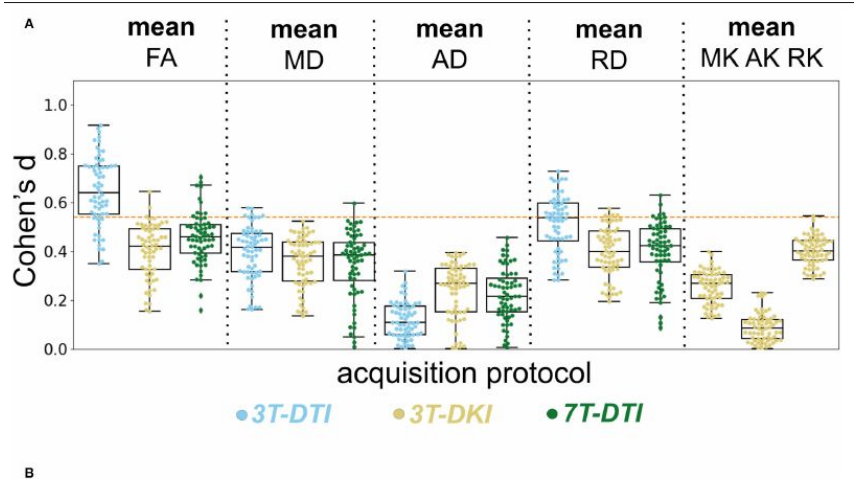

TABLE 1 | Demographics and image acquisition parameters.

Image acquisition	#SLE, #HC	Mean age (std) of HC, SLE	Image resolution (isotropic, in mm^3)	*b*-values in s/mm^2 (# of directions)	TR/TE in ms/ms
3T-DTI	63, 20	37 (9) , 36 (9)	2.0	0 (8), 1,000 (64)	7,300/73
3T-DKI	56, 20	37 (9) , 35 (9)	2.3	0 (3), 250 (6), 500 (6), 1,000 (20), 2750 (30)	7,500/103
7T-DTI	54, 21	40 (10) , 40 (9)	2.0	0 (3), 1,000 (30)	8,816/62

Rows show the three protocols: # corresponds to the number of, SLE, patients with systemic lupus erythematosus; HC, human controls; TR, repetition time; TE, echo time. In total 106 subjects participated in this study: 76 patients with SLE and 30 HC. Out of the 106 subjects, 47 were scanned with all three image acquisition protocols (3T-DTI and 3T-DKI and 7T-DTI): 37 patients with SLE and 10 HC.

Diffusion Tensor and Diffusion Kurtosis Imaging

SLE study

Diffusion protocols & magnetic field strength comparison:

- the **diffusion protocol** had the strongest influence on effect sizes among the ones examined
- **DKI is less sensitive than DTI** to WM pathology in SLE
- FA was the parameter displaying the highest effect sizes in all the protocols.

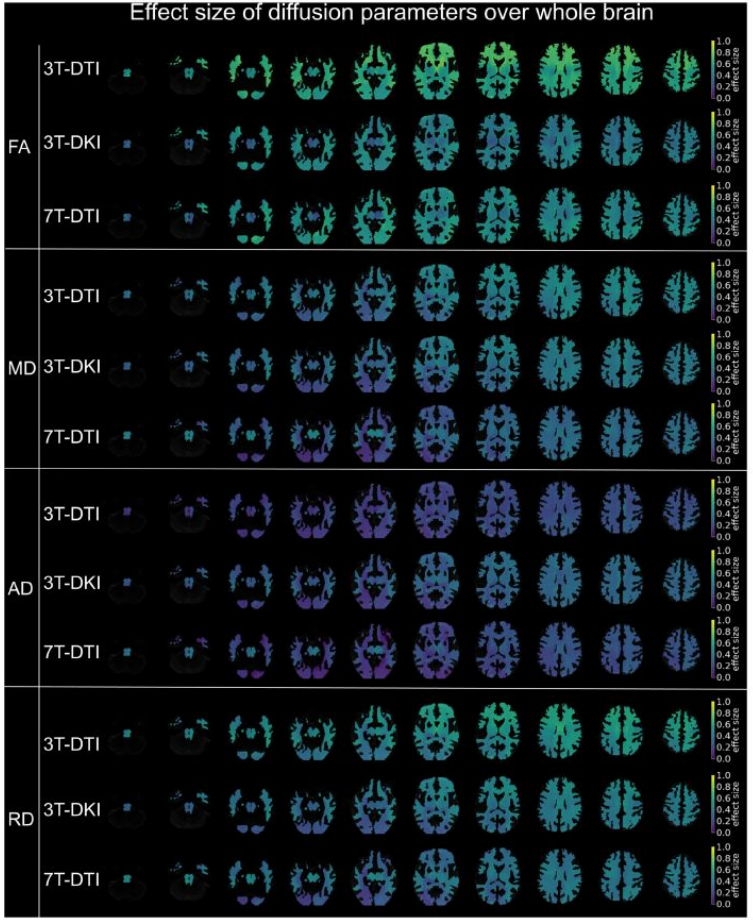

Diffusion Tensor and Diffusion Kurtosis Imaging

SLE study

Diffusion protocols & magnetic field strength comparison:

- the **diffusion protocol** had the strongest influence on effect sizes among the ones examined
- **DKI is less sensitive than DTI** to WM pathology in SLE
- FA was the parameter displaying the highest effect sizes in all the protocols.
- ***no substantial increase in sensitivity came with the use of more demanding acquisitions (DKI and 7T)***

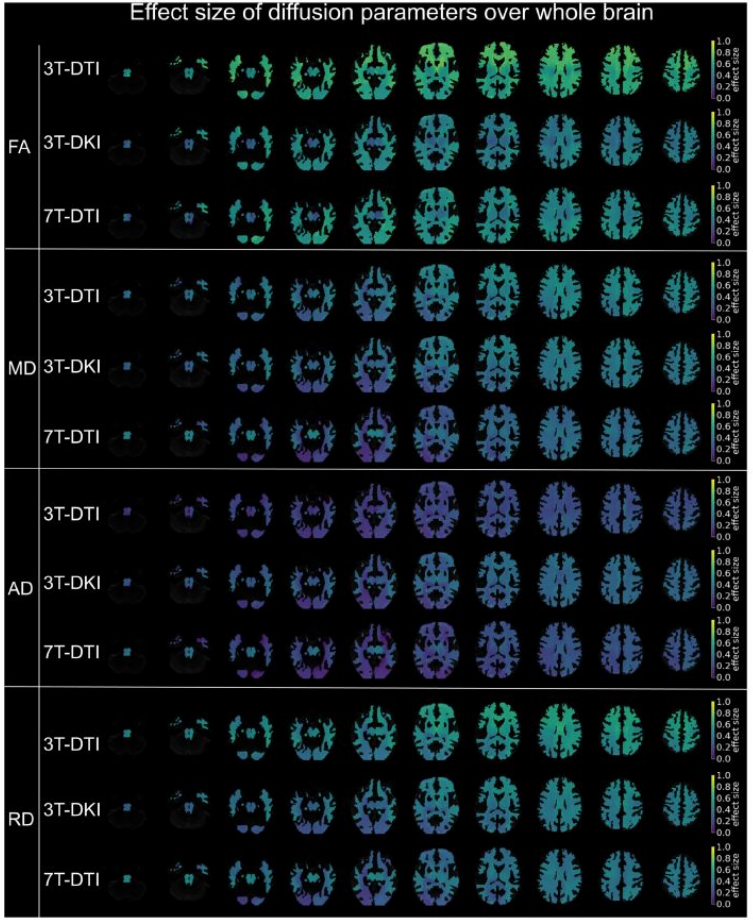

Diffusion Tensor and Diffusion Kurtosis Imaging

SLE study

Diffusion protocols & magnetic field strength comparison:

- the **diffusion protocol** had the strongest influence on effect sizes among the ones examined
- **DKI is less sensitive than DTI** to WM pathology in SLE
- FA was the parameter displaying the highest effect sizes in all the protocols.
- ***no substantial increase in sensitivity came with the use of more demanding acquisitions (DKI and 7T)***

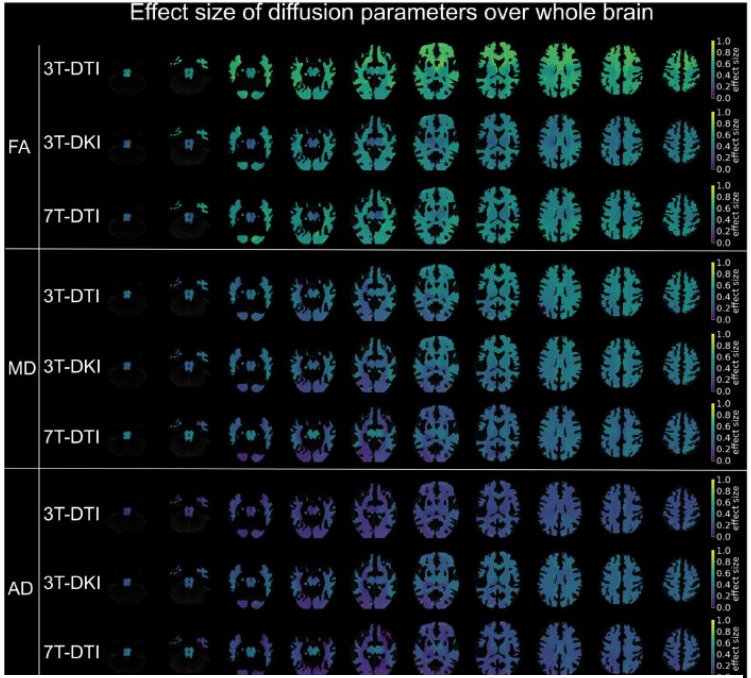

TABLE 1 | Demographics and image acquisition parameters.

Image acquisition	#SLE, #HC	Mean age (std) of HC, SLE	Image resolution (isotropic, in mm^3)	*b*-values in s/mm^2 (# of directions)	TR/TE in ms/ms
3T-DTI	63, 20	37 (9) , 36 (9)	2.0	0 (8), 1,000 (64)	7,300/73
3T-DKI	56, 20	37 (9) , 35 (9)	2.3	0 (3), 250 (6), 500 (6), 1,000 (20), 2750 (30)	7,500/103
7T-DTI	54, 21	40 (10) , 40 (9)	2.0	0 (3), 1,000 (30)	8,816/62

Rows show the three protocols: # corresponds to the number of, SLE, patients with systemic lupus erythematosus; HC, human controls; TR, repetition time; TE, echo time. In total 106 subjects participated in this study: 76 patients with SLE and 30 HC. Out of the 106 subjects, 47 were scanned with all three image acquisition protocols (3T-DTI and 3T-DKI and 7T-DTI): 37 patients with SLE and 10 HC.

Diffusion Tensor and Diffusion Kurtosis Imaging

2 different pathologies in neurodegeneration:

Traumatic Brain Injury (TBI)

Study cohorts & neuroimaging

Athletes, 7T

Healthy controls (N=16)

- Physically active
- M/F:
- Age: 25.5 ± 4.9

Boxers (N=21)

- Active
- MRI ~1month after last match
- M/F: 19/3
- Age: 26.6 ± 6.4

PCPS (N=15)

- PPCS ≥ 6m
- No return to play
- M/F:
- Age: 24.1 ± 4.8

7T MRI (Lund)

- **T1w**
- **T2w**
- **FLAIR**
- **DTI**
- **DKI**

Study cohorts & neuroimaging

Athletes, 7T & PVS computations

7T MRI
(Lund)

- **T1w**
  - FOV: 230×230×180 mm³
  - resolution: 0.80×0.80×0.80 mm³
  - TR/TE: 6/0.39132 ms
- **T2w**
  - FOV: 230×230×180 mm³
  - resolution: 0.80×0.80×0.80 mm³
  - TR/TE: 3.2/0.25 ms
- **FLAIR**
  - FOV: 230×230×180 mm³
  - resolution: 0.70×0.70×0.70 mm³
  - TR/TE: 6/0.39132 ms

- **DTI**
  - FOV: 224×224×110 mm³
  - resolution: 2.00×2.00×2.00 mm³
  - TR/TE: 9200/65 ms
  - 6 b = 100 s/mm²
  - 30 b = 1000 s/mm²
  - TOPUP (2 b = 0 with opposing polarities of the phase-encode blips)

- **DKI**
  - FOV: 224×224×120 mm³
  - resolution: 2.00×2.00×2.00 mm³
  - TR/TE: 9800/76 ms
  - 6 b = 100 s/mm²
  - 6 b = 500 s/mm²
  - 10 b = 1000 s/mm²
  - 30 b = 2000 s/mm²
  - TOPUP (2 b = 0 with opposing polarities of the phase-encode blips)

Study cohorts & neuroimaging

Athletes, 7T & PVS computations

So far 2 publications:

- *Gard, Al-Husseini, Kornaropoulos et al.,* ***Post-concussive vestibular dysfunction is related to injury to the inferior vestibular nerve****, Journal of neurotrauma 39 (11-12), 829-840*
- *Gard, Kornaropoulos et al.,* ***Widespread White Matter Abnormalities in Concussed Athletes Detected by 7T Diffusion Magnetic Resonance Imaging****, Journal of Neurotrauma 41 (13-14), 1533-1549*

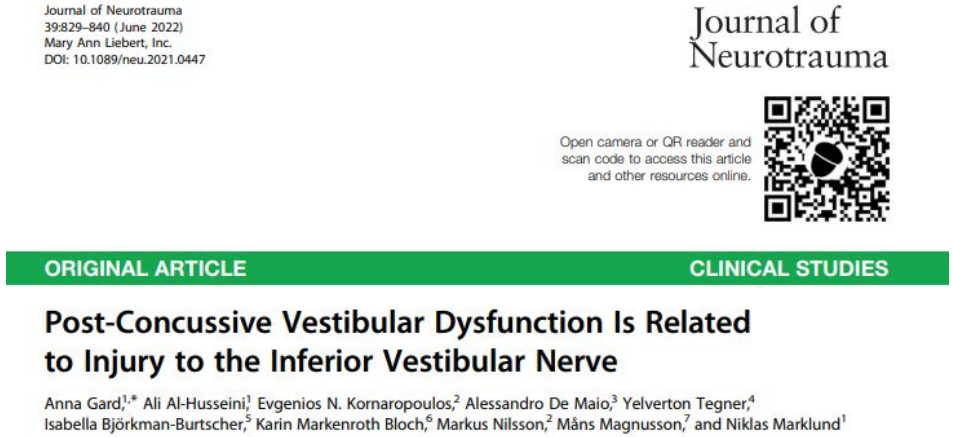

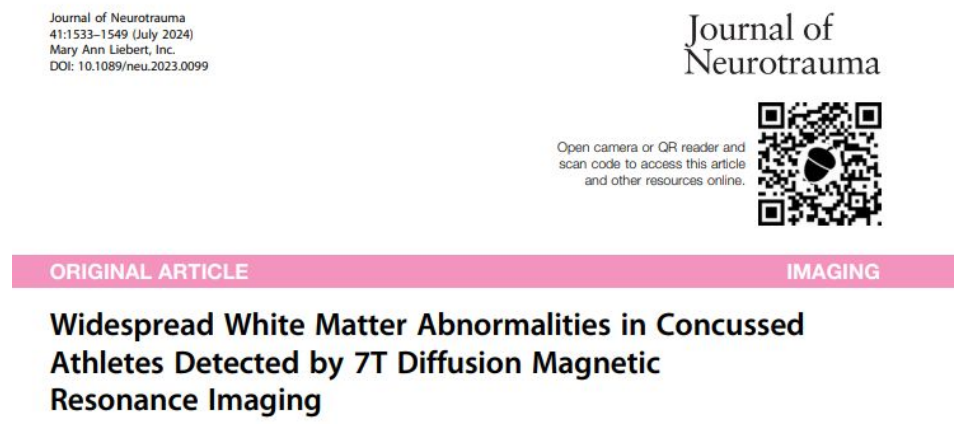

Study cohorts & neuroimaging

Athletes, 7T & PVS computations

So far 2 publications:

- *Gard, Al-Husseini, Kornaropoulos et al.,* ***Post-concussive vestibular dysfunction is related to injury to the inferior vestibular nerve****, Journal of neurotrauma 39 (11-12), 829-840*

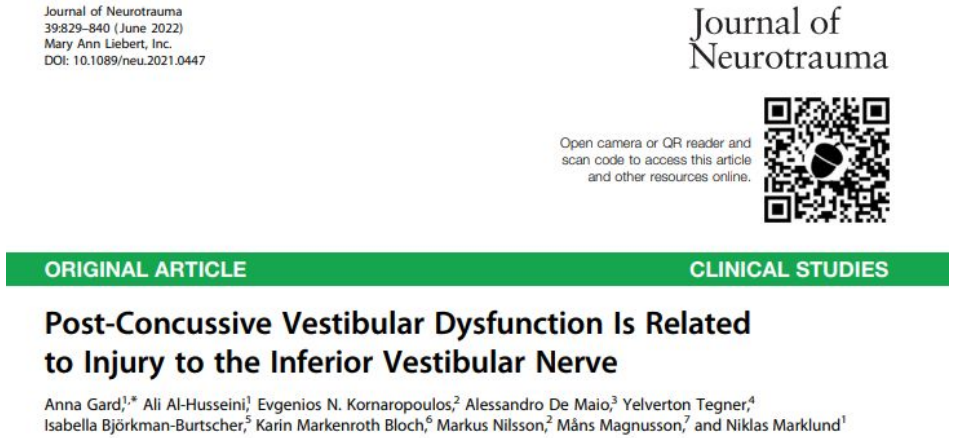

Journal of Neurotrauma
39:829–840 (June 2022)
Mary Ann Liebert, Inc.
DOI: 10.1089/neu.2021.0447

Journal of Neurotrauma

Open camera or QR reader and scan code to access this article and other resources online.

ORIGINAL ARTICLE CLINICAL STUDIES

Post-Concussive Vestibular Dysfunction Is Related to Injury to the Inferior Vestibular Nerve

Anna Gard,[1,*] Ali Al-Husseini,[1] Evgenios N. Kornaropoulos,[2] Alessandro De Maio,[3] Yelverton Tegner,[4] Isabella Björkman-Burtscher,[5] Karin Markenroth Bloch,[6] Markus Nilsson,[2] Måns Magnusson,[7] and Niklas Marklund[1]

- No significant differences in DTI/DKI metrics of cerebellar white matter tracts
- Cerebellar gray and white matter volumes were similar in athletes with SRC and control subjects.

Study cohorts & neuroimaging

Athletes, 7T & PVS computations

So far 2 publications:

- *Gard, Kornaropoulos et al.,* ***Widespread White Matter Abnormalities in Concussed Athletes Detected by 7T Diffusion Magnetic Resonance Imaging****, Journal of Neurotrauma 41 (13-14), 1533-1549*

- Widespread microstructural alterations in the white matter that correlated with CSF markers of axonal injury
- DKI was more sensitive, detecting more white matter changes than DTI

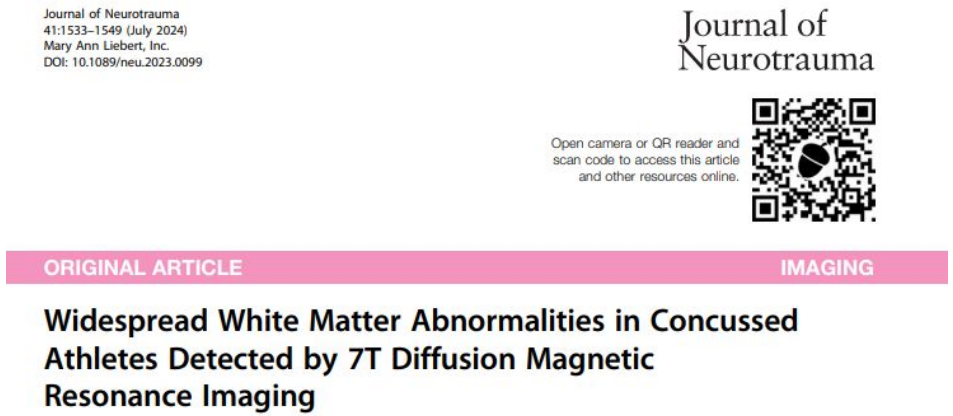

Ongoing project: A proxy for glymphatic system malfunction after mild TBI

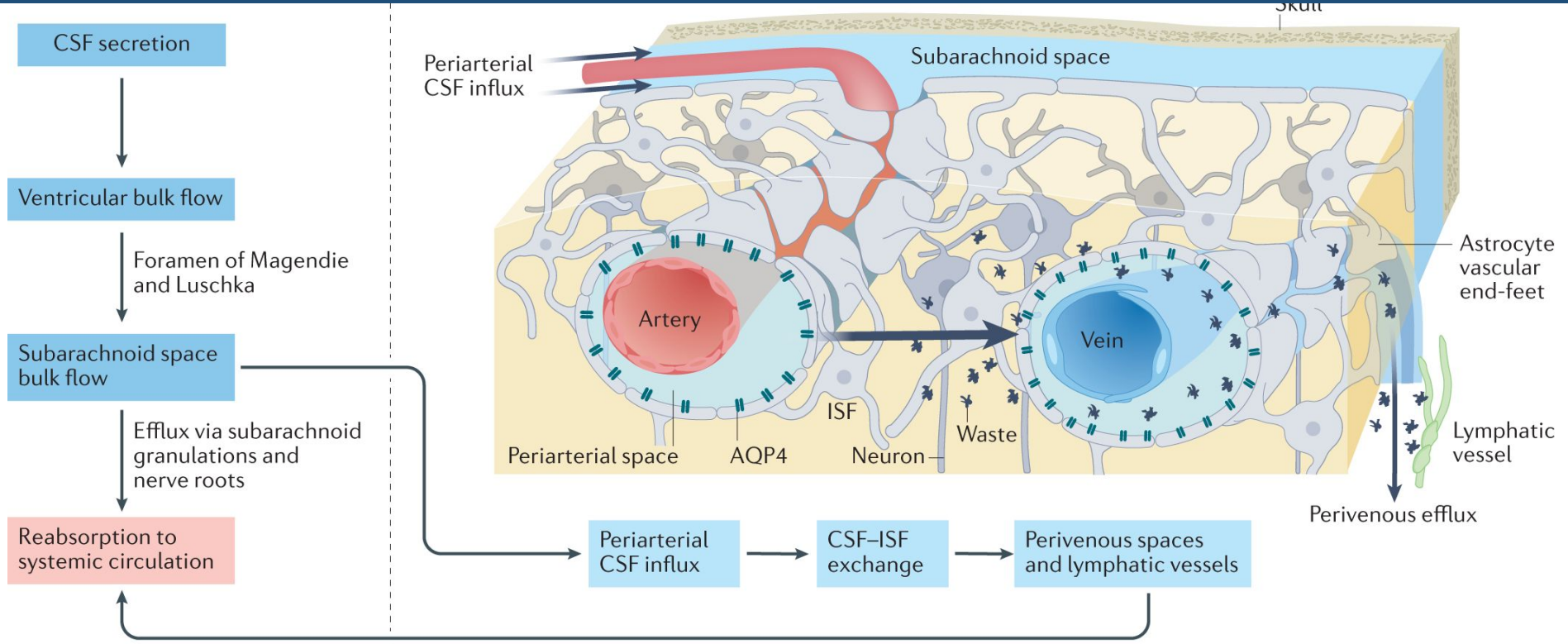

Lohela et al., 2022

Representative PVS masks
3D rendering

PVS automatic method 1: *Sepehrband et al.*

OPEN

Image processing approaches to enhance perivascular space visibility and quantification using MRI

Received: 24 April 2019
Accepted: 15 August 2019
Published online: 26 August 2019

Farshid Sepehrband[1], Giuseppe Barisano[1,2], Nasim Sheikh-Bahaei[1,3], Ryan P. Cabeen[1], Jeiran Choupan[1,4], Meng Law[1,5] & Arthur W. Toga[1]

Imaging the perivascular spaces (PVS), also known as Virchow-Robin space, has significant clinical value, but there remains a need for neuroimaging techniques to improve mapping and quantification of the PVS. Current technique for PVS evaluation is a scoring system based on visual reading of visible PVS in regions of interest, and often limited to large caliber PVS. Enhancing the visibility of the PVS could support medical diagnosis and enable novel neuroscientific investigations. Increasing the MRI resolution is one approach to enhance the visibility of PVS but is limited by acquisition time and physica constraints. Alternatively, image processing approaches can be utilized to improve the contrast ratio between PVS and surrounding tissue. Here we combine T1- and T2-weighted images to enhance PVS contrast, intensifying the visibility of PVS. The Enhanced PVS Contrast (EPC) was achieved by combining T1- and T2-weighted images that were adaptively filtered to remove non-structured high-frequency spatial noise. EPC was evaluated on healthy young adults by presenting them to two expert readers and also through automated quantification. We found that EPC improves the conspicuity of the PVS and aid resolving a larger number of PVS. We also present a highly reliable automated PVS quantification approach, which was optimized using expert readings.

They use EPC after NL means filtering

PVS automatic method 2: *Duarte Coelle et al.*

Journal of Neuroscience Methods 403 (2024) 110039

Contents lists available at ScienceDirect

Journal of Neuroscience Methods

journal homepage: www.elsevier.com/locate/jneumeth

Detectability and accuracy of computational measurements of *in-silico* and physical representations of enlarged perivascular spaces from magnetic resonance images

Roberto Duarte Coello[a], Maria del C. Valdés Hernández[a,*], Jaco J.M. Zwanenburg[b], Moniek van der Velden[b], Hugo J. Kuijf[b], Alberto De Luca[b], José Bernal Moyano[a,c,d], Lucia Ballerini[a,e], Francesca M. Chappell[a], Rosalind Brown[a], Geert Jan Biessels[b], Joanna M. Wardlaw[a]

[a] Centre for Clinical Brain Sciences, Department of Neuroimaging Sciences, University of Edinburgh, Edinburgh, UK
[b] Image Sciences Institute, UMC Utrecht, Utrecht, Netherlands
[c] German Centre for Neurodegenerative Diseases, Magdeburg, Germany
[d] Institute of Cognitive Neurology and Dementia Research, Otto-von-Guericke University Magdeburg, Magdeburg, Germany
[e] University for Foreigner of Perugia, Perugia, Italy

ARTICLE INFO

Keywords:
Perivascular spaces
Virchow-Robin spaces
MRI phantom

ABSTRACT

Background: Magnetic Resonance Imaging (MRI) visible perivascular spaces (PVS) have been associated with age, decline in cognitive abilities, interrupted sleep, and markers of small vessel disease. But the limits of validity of their quantification have not been established.
New method: We use a purpose-built digital reference object to construct an in-silico phantom for addressing this need, and validate it using a physical phantom. We use cylinders of different sizes as models for PVS. We also evaluate the influence of 'PVS' orientation, and different sets of parameters of the two vesselness filters that have been used for enhancing tubular structures, namely Frangi and RORPO filters, in the measurements' accuracy.
Results: PVS measurements in MRI are only a proxy of their true dimensions, as the boundaries of their representation are consistently overestimated. The success in the use of the Frangi filter relies on a careful tuning of several parameters. Alpha= 0.5, beta= 0.5 and c= 500 yielded the best results. RORPO does not have these requirements and allows detecting smaller cylinders in their entirety more consistently in the absence of noise and confounding artefacts. The Frangi filter seems to be best suited for voxel sizes equal or larger than 0.4 mm-isotropic and cylinders larger than 1 mm diameter and 2 mm length. 'PVS' orientation did not affect measurements in data with isotropic voxels.
Comparison with existent methods: Does not apply.
Conclusions: The in-silico and physical phantoms presented are useful for establishing the validity of quantification methods of tubular small structures.

They use Frangi or RORPO filtering

Representative PVS masks

3D rendering

PVS automatic method 1:
Sepehrband et al.

more robust across scanners

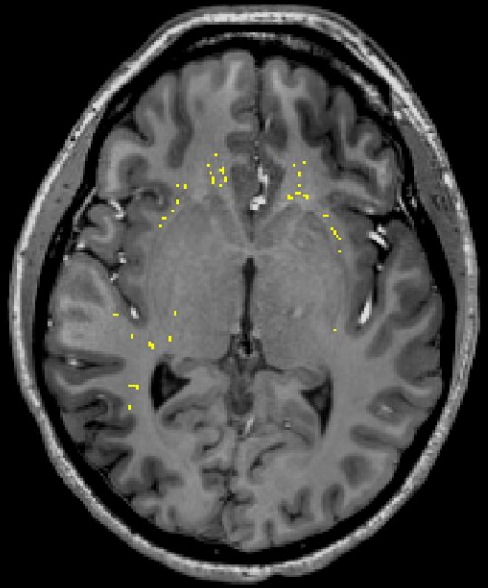

PVS automatic method 2:
Duarte Coelle et al.

more precise for our data

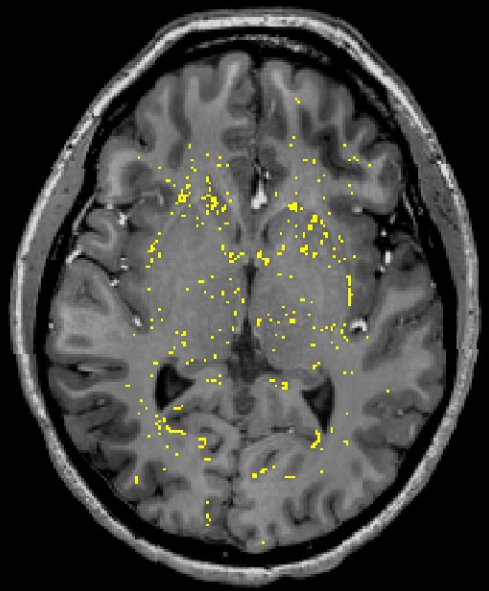

Representative PVS masks

3D rendering

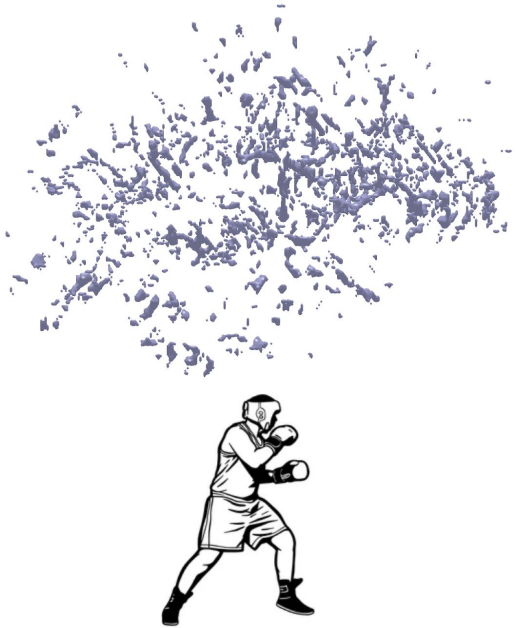

Ongoing collaborations

Multicenter mild TBI dataset for glymphatic measures & correlations

CENTER-TBI

Virginia Newcombe
MD, PhD
Cambridge, UK

David K. Menon
MD, PhD
Co-chair, CENTER-TBI
Cambridge, UK

UNIVERSITY OF CAMBRIDGE

- HC vs Mild TBI
- PVSF & Diffusivity
- Cerebrovascular burden
- Fluid biomarkers
- Cognition

Ongoing collaborations

Department of Neurosurgery, Lund University

Principal Investigator: Professor Niklas Marklund

LUNDS UNIVERSITET

Thank you !

Acknowledgements

Markus Nilsson
Associate Professor,
MR scientist
Lund University

Karin Markenroth Bloch
PhD, MR scientist
Lund University

Anna Gard
PhD, MD, Neurologist,
Lund University

Olivier Girard
PhD, MRI Engineer,
Aix-Marseille University

Guillaume Duhamel
PhD, MRI Physicist,
Aix-Marseille University

LUNDS UNIVERSITET

Aix*Marseille université